BEELEIGH ABBEY, MALDON, ESSEX:
Archaeomagnetic Dating Report 2002

Paul Linford

Summary

A number of medieval buildings were discovered in excavations carried out by the Maldon Archaeological Group in conjunction with the Essex County Council Field Archaeology Unit in a field adjacent to Beeleigh Abbey near Maldon in Essex. Some of the best preserved features in these buildings were a series of tile hearths and the Centre for Archaeology was asked to provide archaeomagnetic analysis for four of these. One of the hearths could not be dated, as its surface had not been exposed to sufficient heat during use. A second hearth from the latest building in the group, a late medieval hall house, was last used in the late C15th AD which is consistent with the archaeological evidence which suggests that the building went out of use around 1530-1540. A third hearth from a smaller building to the north also dated to the same period and it is possible that this building was the kitchen for the hall. The final larger hearth from a building to the west dated to the mid-C13th AD, suggesting that this was the earliest structure so far uncovered at the site.

BEELEIGH ABBEY, MALDON, ESSEX:
Archaeomagnetic Dating Report 2002

Introduction

Beeleigh Abbey, on the outskirts of Maldon on the Essex Coast, was a Premonstratensian house founded at the end of the C12th AD which preserves significant remains of early C13th buildings (TL 850 071, longitude 0.7^{o}E, latitude 51.7^{o}N). During 2002, the Maldon Archaeological Group, in conjunction with the Essex County Council Field Archaeology Unit carried out excavations in an adjacent field, uncovering a well preserved late medieval hall house as well as a series of four earlier, less well preserved houses to the north and west. The late medieval hall can be broadly dated to the C15th AD with no evidence to suggest that it continued in use after the dissolution of the Abbey. The other houses are less well preserved and their dating is more problematic, although they must date from the period between about 1200 and 1400 AD. The stratigraphic relationships between them are not entirely clear and their best preserved features are a series of tile hearths. These are constructed from roof tiles set into the ground so that only the narrow edge of each tile faces upwards. Many such tiles are used, packed close together in parallel, to form the hearth surface.

In view of the suitability of the hearths for archaeomagnetic dating, David Andrews of Essex County Council requested that the English Heritage Centre for Archaeology (EH C*f*A) provide archaeomagnetic analysis of the hearths, to help elucidate the chronology of the site. This request was supported by Deborah Priddy the EH Inspector of Ancient Monuments for the area. Hence, archaeomagnetic sampling was carried out at the site between the 18th and 20th November 2002 by the author with the assistance of David Andrews as well as Bill Clark, Derek Punchard, Alistair Cameron and Pat Ryan of the Maldon Archaeological Group. Four hearths were sampled: one of the three hearths in the late medieval hall house referred to as Building 2; a large central hearth in an earlier house to the west known as Building 3; and two further hearths in smaller houses to the north of Building 2 referred to as Buildings 4 and 5. All subsequent measurements and analyses were carried out by the author. The archaeological information appearing in this report concerning the excavations at Beeleigh Abbey was supplied by Bill Clark and David Andrews, to whom I am grateful.

Method

Samples were collected from the four hearths using the disc method (see appendix, section 1a). Samples from Building 5 were orientated to true north using a gyro-theodolite. The samples from the other three buildings were orientated using a magnetic compass and the deviation between magnetic and true north was established using the International Geomagnetic Reference Field (IGRF 2000). Each hearth was identified using a prefix consisting of the number of the building it was situated in and the letters "BA" (e.g.: all samples from the hearth in Building 5 were prefixed with "5BA"). All samples were of tile and were cut to a suitable size for the measuring equipment using a rock cutting wheel in the laboratory.

The natural remanent magnetisation (NRM) measured in archaeomagnetic samples is assumed to be caused by thermoremanent magnetisation (TRM) created at the time when the feature of which they were part was last fired. However, a secondary component acquired in later geomagnetic fields can also be present, caused by diagenesis or partial reheating. Additionally, the primary TRM may be overprinted by a viscous component, depending on the grain size distribution within the magnetic material. These secondary components are usually of lower stability than the primary TRM and can thus be removed by partial demagnetisation of the samples.

A typical strategy for analysing a set archaeomagnetic samples from a fired archaeological feature is to first measure their NRM magnetisation. These NRM measurements are then inspected and one or more samples are selected for pilot partial demagnetisation. Pilot demagnetisation of a sample involves exposing it to an alternating magnetic field of fixed peak strength and measuring the resulting changes in its magnetisation. The procedure is repeated with increasing peak field strengths to build up a complete picture of the coercivity spectrum of the pilot sample. From these pilot partial demagnetisation results an optimum peak field strength is selected to be applied to the remaining samples. This optimum field strength is chosen to remove as much of the secondary magnetisation as possible whilst leaving the primary magnetisation intact. The equipment used for these measurements is described in section 2 of the appendix.

A mean TRM direction is then calculated from the partially demagnetised sample measurements. Some samples may be excluded from this calculation if their TRM directions are so anomalous as to make them statistical outliers from the overall TRM distribution. A "magnetic refraction" correction is often applied to the sample mean TRM direction to compensate for distortion of the earth's magnetic field due to the geometry of the magnetic fabric of the feature itself. Then the mean is adjusted according to the location of the feature relative to a notional central point in the UK (Meriden), so that it can be compared with UK archaeomagnetic calibration data to produce a date of last firing for the feature. Notes concerning the mean calculation and subsequent calibration can be found in sections 3 and 4 of the appendix.

This measurement and calibration strategy was applied to the analysis of the samples from Beeleigh Abbey. Whilst each of the hearths' constituent tiles was orientated vertically in the ground, a horizontal surface was formed by the top edges of many such tiles packed in close proximity. Only the top edge of each tile will have been significantly heated by the use of the hearth. Hence it was considered that each hearth could be modelled as a continuous horizontal sheet, so a magnetic refraction correction of 2.4^{o} was added to the inclination of each mean TRM direction before calibration (see note 3b).

Results

Table 1 summarises the mean TRM directions and the deduced date ranges for all the features sampled at Beeleigh Abbey. This section provides descriptions of the features sampled and notes any important points about their archaeomagnetic analysis. TRM measurements for all samples may be found grouped by feature in the tables at the end of the report. These tables also record each sample's composition, the demagnetisation level applied to it and whether it was rejected from the feature's mean TRM calculation.

Feature	N	Dec^o	Inc^o	α_{95}	K	Date Range	Comment*
2BA	8	9.4 (8.9)	60.1 (60.6)	2.0	766.4	63%: 1465 – 1495 AD 95%: 1450 – 1505 AD	This was the earliest of several hearths in a late medieval hall thought to have been abandoned at the dissolution. A late C15th date was expected.
3BA	14	11.3 (10.6)	56.4 (56.8)	1.8	471.1	63%: 1240 – 1260 AD 95%: 1225 – 1265 AD	Building 3 pre-dates Building 2 and is thought to date from the C13th – C14th.
4BA	10	7.2 (6.8)	62.0 (62.5)	2.7	314.5	63%: 1475 – 1505 AD 95%: 1445 – 1515 AD	Building 4 was thought to pre-date Building 3 and a date in the C13th was expected.
5BA	-	-	-	-	-	Could not be dated archaeomagnetically.	Expected to pre-date Building 4.

Table 1; Archaeomagnetic dates inferred for tile hearths sampled at Beeleigh Abbey. N = number of samples used to calculate mean TRM. Dec = mean declination (bracketed value is Meriden corrected). Inc = mean inclination (bracketed value is Meriden corrected). α_{95} = internal angle of cone of confidence. k = Fisher precision statistic. *Comment on expected date based upon archaeological considerations.

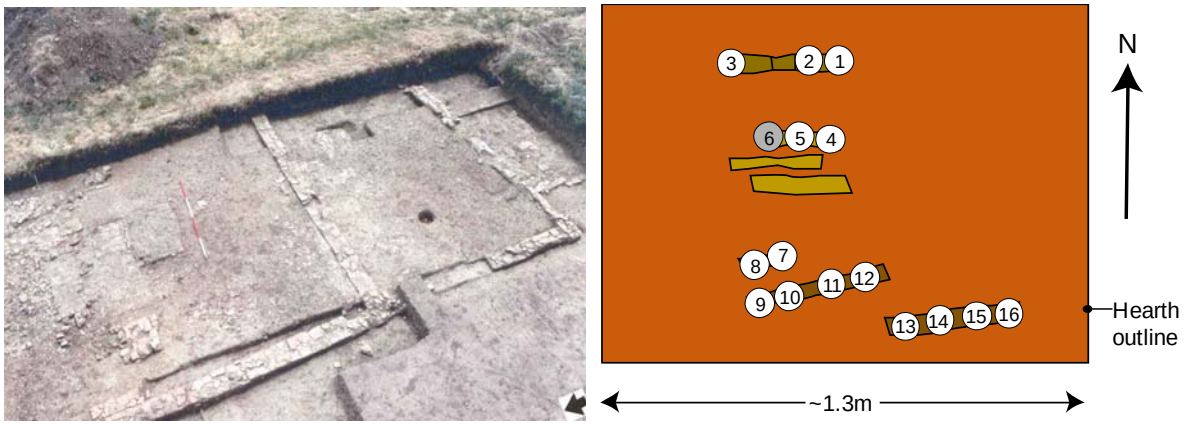

Figure 1: Photograph (left) and sketch plan (right) of the hearth sampled in Building 2. The photograph is viewed from the west and the hearth is immediately to the left of the ranging rod. The sketch shows the approximate distribution of samples (not to scale). Discs shaded grey indicate samples that disintegrated during extraction. Photograph courtesy of William Clark.

Building 2

Building 2 was a late medieval hall house (see Figure 1), which finds and architectural considerations date to the late C15th AD. There was little evidence for any pottery of types in use later than the mid-C16th AD and it is thus assumed that the house was abandoned at the dissolution of the abbey. The hall contained three hearths and it was decided to sample the most central of these for archaeomagnetic dating. Consideration of its position and construction suggested it to be the earliest of the three and an archaeomagnetic date would thus provide a *terminus ante quem* for the first phase of occupation of the building.

The tiles in this hearth were orientated with their long axes east-west. Approximate sample locations are depicted in the right hand part of Figure 1. Sample disc 6 failed to adhere properly and was lost during extraction. Sample measurements are recorded in Tables 2 and 3 and Figure 5 depicts the distribution of sample TRM directions before and after partial demagnetisation. Figures 6 to 8 illustrate the results of pilot demagnetisation on samples 2BA01, 2BA07 and 2BA10 respectively.

Table 4 shows stability estimates for the magnetisation in these samples based upon the method of Tarling and Symons (1967). In this method, any sample with a maximum stability parameter greater than 2 is judged to record a stable TRM direction and a parameter value over 5 suggests extreme stability. The figures in Table 4 indicate that the magnetisations of all three pilot demagnetisation samples are extremely stable, with the maximum stabilities occurring between 1 and 20mT. As sample 2BA10 exhibited some instability in domains with coercivities up to 10mT, it was decided to partially demagnetise the remaining samples in a 15mT AF field.

The distribution of TRM directions after this treatment is depicted in Figure 5b. It can be seen that samples 2BA13-16 all have TRM directions that fall outside the main cluster, even after this treatment. These four samples all came from the same tile and all had relatively low intensities of magnetisation. It was concluded that this tile had not experienced sufficiently high temperatures to realign their directions of magnetisation during the use of the hearth. Hence, these samples were rejected from the calculation of the mean TRM.

Samples 2BA01-02 and 2BA10, although closer to the main cluster, also fall outside it. These three samples all came from parts of tiles that had broken up due to the heat that they had been exposed to. This was not apparent until the latter stages of sampling when the tiles were extracted, when the parts containing these samples broke away. It was concluded that these samples may thus have been disturbed during the excavation of the feature and they were also excluded from the mean TRM calculation. A mean TRM direction was calculated using the measurements made on the remaining 8 samples (see note 3) and it is depicted in Figure 9 superimposed on the UK archaeomagnetic calibration curve. A date range for the last firing of the hearth was deduced from this mean (note 4) and this is quoted in Table 1. It should be noted that at 95% confidence a date range in the late C13th is also possible but this is not quoted as archaeological considerations preclude such an early date.

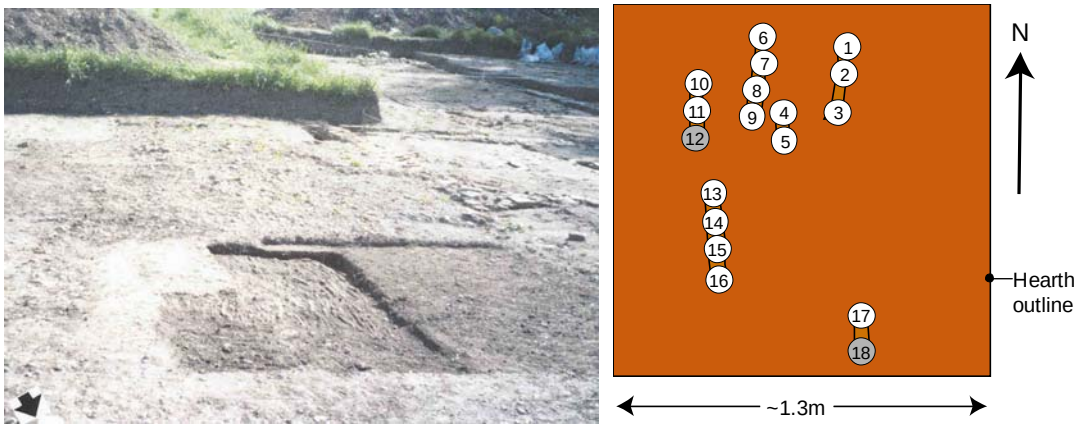

Figure 2: Photograph (left) and sketch plan (right) of the hearth sampled in Building 3. The photograph is viewed from the north and the hearth visible in the central foreground. The sketch shows the approximate distribution of samples (not to scale). Discs shaded grey indicate samples that disintegrated during extraction. Photograph courtesy of William Clark.

Building 3

Building 3 appears to have been a precursor to Building 2, enclosing a similar area but with walls constructed of tiles stacked at an angle rather than laid flat. It lies to the northeast of Building 2 and is thought to date from the C13th–14th AD. It contains a large central hearth constructed of tiles stacked vertically with their long axes aligned north-south. Approximate sample locations are depicted in the right hand part of Figure 2. Sample discs 12 and 18 failed to adhere properly and were lost during extraction. Sample measurements are recorded in Tables 5 to 7 and Figure 10 depicts the distribution of sample TRM directions before and after partial demagnetisation. Figures 11 to 14 illustrate the results of pilot demagnetisation on samples 3BA08, 3BA10, 3BA14 and 3BA16 respectively.

Table 8 shows stability estimates for the magnetisation in these samples based upon the method of Tarling and Symons (1967). The figures in Table 8 indicate that the magnetisations of all three pilot demagnetisation samples are extremely stable, with the maximum stabilities occurring between about 10 and 30mT. Sample 3BA14 exhibits a secondary component of magnetisation in domains with coercivities below 30mT. However, sample 3BA16 from the same tile does not contain this component and it was concluded that the behaviour of sample 3BA14 was an isolated anomaly. After consideration of the pilot demagnetisation results, it was decided to partially demagnetise the remaining samples in a 15mT AF field.

The distribution of TRM directions after this treatment is depicted in Figure 10b. It can be seen that samples 3BA10-11 all have TRM directions that fall outside the main cluster, even after this treatment. These two samples both came from the same tile and it was concluded that this tile had been disturbed since the last firing of the hearth. Hence, these two samples were rejected from the calculation of the mean TRM direction which was calculated using the measurements made on the remaining 14 samples (see note 3). It is depicted in Figure 15 superimposed on the UK archaeomagnetic calibration curve. A date range for the last firing of the hearth was deduced from this mean (note 4) and this is quoted in Table 1.

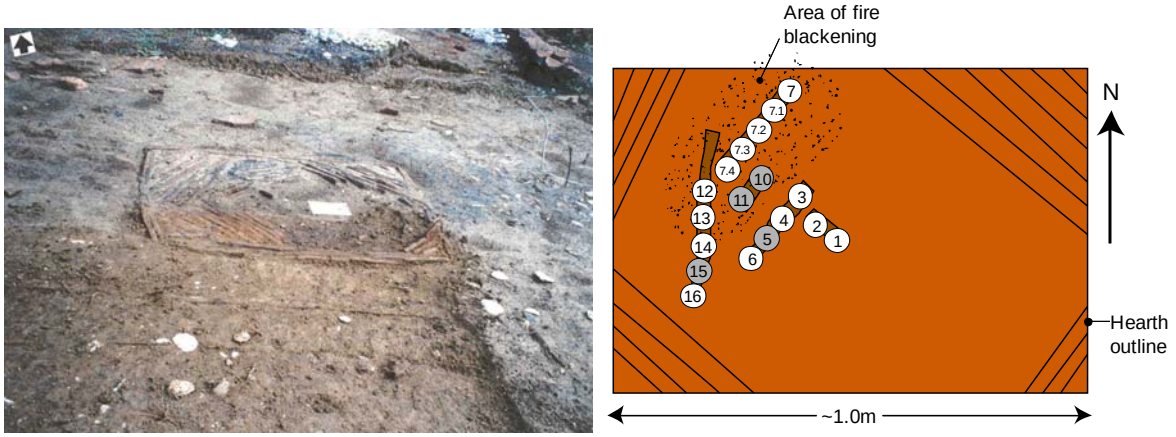

Figure 3: Photograph (left) and sketch plan (right) of the hearth sampled in Building 4. The photograph is viewed from the south. The sketch shows the approximate distribution of samples (not to scale). Discs shaded grey indicate samples that disintegrated during extraction Note that samples 08 and 09 also failed but these were replaced in the laboratory by samples 7.1-7.4, the positions of which are indicated. Photograph courtesy of William Clark.

Building 4

Building 4 was a smaller structure due north of Building 2. It was thought to predate building 3 and thus to date from the C13th AD. Within the building was a hearth similar to those in Buildings 2 and 3 but slightly smaller in size, measuring about 1m across its longest dimension. It also differed from the other hearths on the site in the arrangement of its constituent tiles, which were laid diagonally to form a lozenge shape (Figure 3).

Approximate sample locations are depicted in the right hand part of Figure 3. Sample discs 05, 08-11 and 15 were lost during extraction. However, the tile containing samples 07-09 was subsampled in the laboratory using orientation information from the remaining sample disc (07), to provide the additional four samples, 07.1-07.4. Sample measurements are recorded in Tables 9 and 10 and Figure 16 depicts the distribution of sample TRM directions before and after partial demagnetisation. Figures 17 to 19 illustrate the results of pilot demagnetisation on samples 4BA01, 4BA07.2 and 4BA07.3 respectively.

Table 11 shows stability estimates for the magnetisation in these samples based upon the method of Tarling and Symons (1967). The figures in Table 11 indicate that the magnetisations of all three pilot demagnetisation samples are extremely stable, with the maximum stabilities occurring between about 10 and 20mT. Thus, after consideration of the pilot demagnetisation results, it was decided to partially demagnetise the remaining samples in a 15mT AF field.

The distribution of TRM directions after this treatment is depicted in Figure 16b. It can be seen that samples 4BA07, 4BA07.3, 4BA07.4 and 4BA16 all have TRM directions that fall outside the main cluster, even after this treatment. It is not immediately clear why this should be so, as all four samples came from intact tiles that also contained samples possessing TRM directions that do fall within the main cluster. It was concluded that the pattern of use of this hearth must have lead to relatively inconsistent heating of its surface, perhaps due to accumulations of ash. These four samples were rejected from the calculation of the mean TRM direction which was calculated using the measurements made on the remaining 10 samples (see note 3). It is depicted in Figure 20 superimposed on the UK archaeomagnetic calibration curve. A date range for the last firing of the hearth was deduced from this mean (note 4) and this is quoted in Table 1.

The derived date range falls in the late C15th AD but it should be noted that, at 95% confidence, date ranges in the late C12th or C13th AD are also possible. However, the mean TRM direction of hearth 2BA lies between 4BA's mean and these earlier segments of the calibration curve (see the grey cross in Figure 20). On archaeological grounds, 2BA dates from no earlier than the C15th AD. As 4BA's mean TRM direction lies further from the C12th–C13th AD segment of the calibration curve than 2BA's mean, it is extremely unlikely that the former should be interpreted as indicating a date in this earlier period.

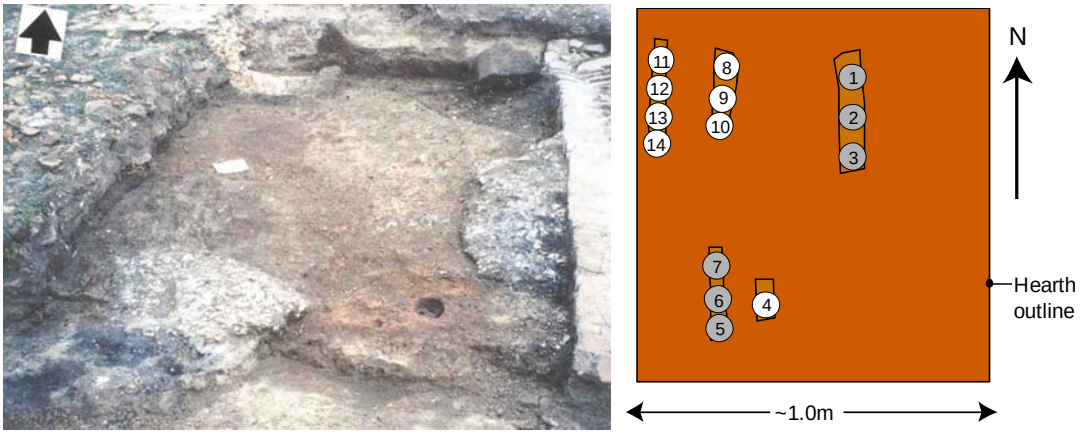

Figure 4: Photograph (left) and sketch plan (right) of the hearth sampled in Building 5. The photograph is viewed from the south and the hearth visible in the left foreground in front of the white card. The sketch shows the approximate distribution of samples (not to scale). Discs shaded grey indicate samples that disintegrated during extraction. Photograph courtesy of William Clark.

Building 5

Building 5 lies immediately north of Building 4 and is thought to be the earliest structure so far excavated. It contains a large central hearth of similar size to that in Building 4, constructed of tiles stacked vertically with their long axes aligned north-south. Approximate sample locations are depicted in the right hand part of Figure 4. Sample discs 01-03 and 05-07 were lost during extraction. However, the parts of the tiles adjacent to samples 5BA04, 5BA09, 5BA10 and 5BA14 were subsampled in the laboratory to provide the additional samples 5BA04.1, 5BA09.1, 5BA10.1 and 5BA14.1. Sample measurements are recorded in Tables 12 and 13 and Figure 21 depicts the distribution of sample TRM directions before and after partial demagnetisation. Figure 22 illustrates the results of pilot demagnetisation on sample 5BA10.

It is immediately clear from Figure 21 that the NRM directions of all the samples from any particular tile all form a tight cluster. However, the clusters for each tile do not coincide and are randomly positioned in different parts of the stereographic plot. This pattern suggests that the tiles have not been heated sufficiently after incorporation into the hearth to realign their magnetisation directions. The magnetisation directions present in the tiles relate to their date of manufacture. As the tiles have been moved since then, these directions are essentially random. As confirmation, the pilot demagnetisation results from sample 5BA10 show that it has a stable TRM, thus the scatter of sample directions is not due to perturbation by extremely strong secondary or viscous component. It was thus concluded that the pattern of use of the hearth in building 5 was such that its floor was never subjected to high temperatures, perhaps because the fire was contained in a grate above it. Unfortunately, the hearth cannot, therefore, be dated archaeomagnetically.

Conclusions

Archaeomagnetic analysis has successfully deduced dates for the last firing of three of the four hearths sampled at Beeleigh Abbey. The date for the hearth in Building 2 suggests that the hearth was last used in the latter half of the C15th AD. As this is the earliest of three hearths in a late medieval hall thought to have been abandoned at the time of the dissolution of the Abbey, this date is in keeping with expectation. The hearth in Building 3 appears to

have last been used in the mid-C13th AD. This is somewhat surprising as this building is thought to have been the immediate precursor to Building 2 and thus might have been expected to have gone out of use more recently that the C13th AD. However, analysis of the dimensions of Building 3 indicate that it had about twice the floor area of Building 2 and thus an aisled hall structure would have been required to support its roof. Examples of aisled halls dating from the C13th AD are known, so the archaeomagnetic date is not necessarily anomalous.

Most surprising was the date for the hearth in Building 4. Stratigraphically, this building appears to underlie Building 3. The hearth associated with it should therefore produce a date earlier that that of the hearth in the latter building. However, the archaeomagnetic date for the last use of the hearth in Building 4 is in the late C15th AD, contemporary with Building 2. It is possible that this hearth has been disturbed since it was last fired: a southwestward tilt of about 6° could displace a mean TRM direction from the C13th to the C15th segment of the calibration curve. Nevertheless, the stratigraphic relationships between the various structures in this part of the site have yet to be fully examined and so, on present evidence, this archaeomagnetic date cannot be categorically ruled impossible. Furthermore, the hearth is situated immediately north of Building 2 and this area could well be the (as yet unidentified) kitchen building for it. In this case a contemporary date would be quite consistent.

The fourth hearth, in Building 5, could not be dated by archaeomagnetic analysis. Owing to difficulties in extracting the tightly packed tiles from this feature, only three separate tiles were sampled. None of these showed any indication of realignment of the magnetisation that they had acquired during manufacture. This suggests that they had not experienced heating to above ~200°C during the use of the hearth. It is possible that this is due to misfortune and that, had further tiles been sampled, a TRM produced by the firing of the hearth would have been identified. However, given that the 3 tiles sampled came from different parts of the feature, this seems unlikely, particularly in the light of the successful dating of the other three hearths. It is thus possible that the fire in this hearth was held above its surface in a grate.

In the light of the above discussion, it will be interesting to compare the archaeomagnetic dates from Beeleigh Abbey with the chronology derived from other archaeological evidence, both that already recovered and that revealed by proposed further excavation by the Maldon Archaeological Group.

P. Linford
Archaeometry Branch,
Centre for Archaeology, English Heritage.

Date of report: 03/12/2002

Archaeomagnetic Date Summary

Archaeomagnetic ID:	**2BA**
Feature:	**Beeleigh Abbey, Building 2**
Location:	**Longitude 0.7°E, Latitude 51.7°N**
Number of Samples (taken/used in mean):	**15/8**
AF Demagnetisation Applied:	**15mT**
Distortion Correction Applied:	**+2.4 °**
Declination (at Meriden):	**9.4° (8.9°)**
Inclination (at Meriden):	**60.1° (60.6 °)**
Alpha-95:	**2.0°**
k:	**766.4**
Date range (63% confidence):	**1465 AD to 1495 AD**
Date range (95% confidence):	**1450 AD to 1505 AD**
Independent date estimate:	**1400 to 1500 AD**

Archaeomagnetic ID:	**3BA**
Feature:	**Beeleigh Abbey, Building 3**
Location:	**Longitude 0.7°E, Latitude 51.7°N**
Number of Samples (taken/used in mean):	**16/14**
AF Demagnetisation Applied:	**15mT**
Distortion Correction Applied:	**+2.4 °**
Declination (at Meriden):	**11.3° (10.6°)**
Inclination (at Meriden):	**56.4° (56.8 °)**
Alpha-95:	**1.8°**
k:	**471.1**
Date range (63% confidence):	**1240 AD to 1260 AD**
Date range (95% confidence):	**1225 AD to 1265 AD**
Independent date estimate:	**1200 to 1400 AD**

Archaeomagnetic ID:	**4BA**
Feature:	**Beeleigh Abbey, Building 4**
Location:	**Longitude 0.7°E, Latitude 51.7°N**
Number of Samples (taken/used in mean):	**14/10**
AF Demagnetisation Applied:	**15mT**
Distortion Correction Applied:	**+2.4 °**
Declination (at Meriden):	**7.2° (6.8°)**
Inclination (at Meriden):	**62.0° (62.5 °)**
Alpha-95:	**2.7°**
k:	**314.5**
Date range (63% confidence):	**1475 AD to 1505 AD**
Date range (95% confidence):	**1445 AD to 1525 AD**
Independent date estimate:	**1200 to 1400 AD**

Archaeomagnetic ID:	**5BA**
Feature:	**Beeleigh Abbey, Building 5**
Location:	**Longitude 0.7^{o}E, Latitude 51.7^{o}N**
Number of Samples (taken/used in mean):	**12/-**
AF Demagnetisation Applied:	**-**
Distortion Correction Applied:	**-**
Declination (at Meriden):	**-**
Inclination (at Meriden):	**-**
Alpha-95:	**-**
k:	**-**
Date range (63% confidence):	**undatable**
Date range (95% confidence):	**undatable**
Independent date estimate:	**1200 to 1400 AD**

	NRM Measurements				After Partial Demagnetisation			
Sample	Material	Dec°	Inc°	J(mAm^{-1})	AF(mT)	Dec°	Inc°	J(mAm^{-1})	R
2BA01	tile	-6.0	71.4	16325.2	15.0	-7.8	70.2	13885.0	R
2BA02	tile	6.6	69.4	17522.6	15.0	0.5	69.3	13911.2	R
2BA03	tile	8.2	58.8	8562.6	15.0	7.8	57.4	7005.2	
2BA04	tile	7.2	58.3	5334.1	15.0	6.7	57.3	4471.9	
2BA05	tile	3.5	59.3	6532.0	15.0	4.5	58.1	5194.6	
2BA07	tile	10.7	56.9	1041.2	15.0	10.8	55.9	794.5	
2BA08	tile	9.3	60.7	1058.4	15.0	12.2	59.7	842.0	
2BA09	tile	18.4	60.3	2466.2	15.0	21.2	59.3	2078.7	
2BA10	tile	29.7	60.9	1477.4	15.0	34.3	59.4	1186.9	R
2BA11	tile	6.8	57.7	1355.9	15.0	6.9	57.1	1234.4	
2BA12	tile	4.6	57.1	2250.8	15.0	6.2	56.4	2055.8	
2BA13	tile	-48.5	19.4	337.0	15.0	-59.9	-21.4	193.8	R
2BA14	tile	-72.7	-20.3	929.9	15.0	-82.2	-38.1	840.6	R
2BA15	tile	-56.7	-0.7	675.3	15.0	-65.0	-20.1	642.2	R
2BA16	tile	-15.1	48.2	492.6	15.0	-20.5	36.5	307.7	R

Table 2: NRM measurements of samples and measurements after partial AF demagnetisation for feature 2BA. J = magnitude of magnetisation vector; AF = peak alternating field strength of demagnetising field; R = sample rejected from mean calculation.

	2BA01			2BA07			2BA10		
AF(mT)	Dec°	Inc°	J(mAm^{-1})	Dec°	Inc°	J(mAm^{-1})	Dec°	Inc°	J(mAm^{-1})
0.0	-6.4	69.7	17412.4	11.2	57.0	1019.3	30.5	60.1	1481.6
1.0	-7.4	69.5	17342.4	11.0	56.7	1012.7	30.4	59.9	1471.9
2.5	-7.5	69.5	17275.7	10.7	56.6	1002.1	31.0	60.1	1465.2
5.0	-7.3	69.6	16988.1	10.8	56.6	978.5	30.9	60.4	1428.2
10.0	-7.7	69.7	15785.5	10.9	55.9	901.3	32.5	59.5	1328.9
15.0	-7.8	70.2	13885.0	10.8	55.9	794.5	34.3	59.4	1186.9
20.0	-8.4	70.4	11741.0	11.3	55.8	686.7	36.9	58.7	1029.9
30.0	-9.3	71.0	9028.0	12.1	55.5	475.8	40.2	58.3	755.9
50.0	-8.5	71.8	5098.9	16.4	54.4	212.0	41.4	57.8	392.1
75.0	-11.8	69.8	2203.5	37.8	50.2	72.1	56.0	60.3	197.4

Table 3: Incremental partial demagnetisation measurements for samples 2BA01, 2BA07 and 2BA10.

Sample	Range min. (mT)	Range max. (mT)	Max. Stability	Dec°	Inc°
2BA01	1.0	5.0	93.7	-4.8	69.5
2BA07	10.0	20.0	62.8	13.6	55.9
2BA10	0.0	5.0	28.0	33.3	60.1

Table 4: Assessment of the range of demagnetisation values over which each sample attained its maximum directional stability for feature 2BA, using the method of Tarling and Symons (1967). The declination and inclination values quoted are for the mean TRM direction for the sample calculated for all demagnetisation measurements in its range of maximum stability.

	NRM Measurements				After Partial Demagnetisation			
Sample	Material	Dec°	Inc°	J(mAm^{-1})	AF(mT)	Dec°	Inc°	J(mAm^{-1})	R
3BA01	tile	7.5	56.5	703.4	15.0	8.7	55.4	306.6	

3BA02	tile	5.6	53.3	2787.3	15.0	5.0	51.7	1326.7	
3BA03	tile	8.9	55.2	4463.7	15.0	8.1	51.4	1248.2	
3BA04	tile	8.5	57.7	8034.6	15.0	8.1	57.7	7121.9	
3BA05	tile	5.5	57.7	9624.2	15.0	7.0	57.5	8327.4	
3BA06	tile	15.7	51.6	96.2	15.0	19.3	50.4	56.7	
3BA07	tile	11.8	58.6	184.3	15.0	13.6	56.0	123.2	
3BA08	tile	12.5	55.8	1034.4	15.0	12.3	54.7	792.1	
3BA09	tile	10.9	56.7	2133.9	15.0	11.8	55.3	1597.3	
3BA10	tile	25.4	59.6	192.7	15.0	28.4	57.9	117.3	R
3BA11	tile	23.3	59.4	135.0	15.0	29.3	57.9	82.6	R
3BA13	tile	16.4	55.6	2331.6	15.0	15.5	53.1	1932.3	
3BA14	tile	12.9	50.8	2501.9	15.0	12.2	49.9	2215.1	
3BA15	tile	14.0	50.7	2619.1	15.0	14.6	50.5	2359.0	
3BA16	tile	10.9	53.0	2773.7	15.0	11.7	52.3	2495.5	
3BA17	tile	7.0	56.8	750.3	15.0	8.3	59.3	308.3	

Table 5: NRM measurements of samples and measurements after partial AF demagnetisation for feature 3BA. J = magnitude of magnetisation vector; AF = peak alternating field strength of demagnetising field; R = sample rejected from mean calculation.

	3BA08			3BA10		
AF(mT)	Dec°	Inc°	J(mAm^{-1})	Dec°	Inc°	J(mAm^{-1})
0.0	12.5	56.1	1035.1	25.7	60.1	191.0
1.0	12.4	55.8	1030.5	25.8	59.2	184.3
2.5	12.0	55.5	1018.0	26.0	58.9	175.7
5.0	11.8	55.3	992.3	26.7	58.4	159.3
10.0	12.2	55.0	906.3	28.1	57.9	131.4
15.0	12.3	54.7	792.1	28.4	57.9	117.3
20.0	12.0	54.4	654.1	28.0	57.8	108.9
30.0	12.7	53.2	435.4	28.4	57.9	98.1
50.0	13.0	54.0	227.0	28.6	57.8	82.0
75.0	15.5	52.9	131.8	28.0	56.5	74.7

Table 6: Incremental partial demagnetisation measurements for samples 3BA08 and 3BA10.

AF(mT)	3BA14			3BA16		
	Dec°	Inc°	J(mAm^{-1})	Dec°	Inc°	J(mAm^{-1})
0.0	12.7	51.3	2544.6	12.5	53.0	2776.3
1.0	12.4	50.9	2503.8	12.5	52.7	2753.6
2.5	12.3	50.9	2483.8	12.2	52.9	2756.6
5.0	12.6	51.3	2481.6	12.2	52.6	2715.2
10.0	12.2	50.6	2361.3	12.2	52.5	2624.2
15.0	12.2	49.9	2215.1	11.7	52.3	2495.5
20.0	12.5	50.3	2104.1	11.8	52.1	2335.5
30.0	12.3	49.5	1797.0	12.1	51.3	1998.0
50.0	12.3	48.4	1161.9	12.1	51.3	1328.3
75.0	12.5	48.5	677.5	10.8	50.3	761.7
100.0	12.6	44.5	410.2	9.2	48.3	451.2

Table 7: Incremental partial demagnetisation measurements for samples 3BA14 and 3BA16.

Sample	Range min. (mT)	Range max. (mT)	Max. Stability	Dec°	Inc°
3BA08	10.0	20.0	32.0	12.2	54.7
3BA10	10.0	50.0	141.5	28.3	57.9
3BA14	30.0	75.0	34.6	12.4	48.8
3BA16	1.0	10.0	49.0	12.3	52.7

Table 8: Assessment of the range of demagnetisation values over which each sample attained its maximum directional stability for feature 3BA, using the method of Tarling and Symons (1967). The declination and inclination values quoted are for the mean TRM direction for the sample calculated for all demagnetisation measurements in its range of maximum stability.

	NRM Measurements				After Partial Demagnetisation			
Sample	Material	Dec°	Inc°	J(mAm^{-1})	AF(mT)	Dec°	Inc°	J(mAm^{-1})	R
4BA01	tile	-2.4	55.2	4509.1	15.0	-2.4	53.6	2905.6	
4BA02	tile	-0.1	59.8	3800.4	15.0	-1.1	60.4	2577.3	
4BA03	tile	11.5	59.8	1146.9	15.0	11.2	58.3	641.9	
4BA04	tile	8.7	60.0	1082.7	15.0	8.2	59.9	547.1	
4BA06	tile	3.4	59.3	755.2	15.0	2.0	57.8	420.5	
4BA07	tile	35.9	47.7	990.8	15.0	30.6	50.0	708.7	R
4BA07.1	tile	15.2	60.3	993.2	15.0	13.6	59.8	798.2	
4BA07.2	tile	12.1	60.4	333.5	15.0	15.2	59.9	255.9	
4BA07.3	tile	31.6	55.1	312.4	15.0	33.6	52.8	231.9	R
4BA07.4	tile	30.6	62.5	397.6	15.0	38.6	62.9	276.1	R
4BA12	tile	12.1	57.9	1619.8	15.0	14.5	57.4	1290.4	
4BA13	tile	10.6	61.8	2185.0	15.0	10.1	61.1	1419.3	
4BA14	tile	2.6	67.0	1550.9	15.0	1.0	66.4	760.3	
4BA16	tile	-4.7	70.2	328.8	15.0	-21.4	77.0	169.7	R

Table 9: NRM measurements of samples and measurements after partial AF demagnetisation for feature 4BA. J = magnitude of magnetisation vector; AF = peak alternating field strength of demagnetising field; R = sample rejected from mean calculation.

	4BA01			4BA07.2			4BA07.3		
AF(mT)	Dec°	Inc°	J(mAm^{-1})	Dec°	Inc°	J(mAm^{-1})	Dec°	Inc°	J(mAm^{-1})
0.0	-2.1	53.7	4617.2	14.8	60.4	333.0	32.0	55.2	315.2
1.0	-2.8	51.6	4584.6	15.3	60.4	331.2	32.3	54.8	310.7
2.5	-1.9	54.0	4428.2	13.6	60.3	329.5	32.4	54.5	307.4
5.0	-2.1	53.9	4313.0	14.9	60.1	318.5	32.9	53.9	295.2
10.0	-2.2	53.9	3708.8	15.2	59.8	291.2	33.8	53.1	264.9
15.0	-2.4	53.6	2905.6	15.2	59.9	255.9	33.6	52.8	231.9
20.0	-2.3	53.7	2444.5	15.5	59.9	219.7	33.5	52.4	199.1
30.0	-1.9	53.6	1908.0	17.4	58.9	150.8	34.6	50.2	145.2
50.0	-3.7	53.6	1251.9	32.0	57.1	53.2	38.0	35.1	67.6
75.0	-2.8	52.8	682.4	50.0	34.1	17.5	48.6	13.3	35.3

Table 10: Incremental partial demagnetisation measurements for samples 4BA01, 4BA7 and 4BA7.

Sample	Range min. (mT)	Range max. (mT)	Max. Stability	Dec°	Inc°
4BA01	5.0	30.0	83.4	-2.2	53.7
4BA07.2	10.0	20.0	95.9	15.3	59.9
4BA07.3	10.0	20.0	27.5	33.6	52.8

Table 11: Assessment of the range of demagnetisation values over which each sample attained its maximum directional stability for feature 4BA, using the method of Tarling and Symons (1967). The declination and inclination values quoted are for the mean TRM direction for the sample calculated for all demagnetisation measurements in its range of maximum stability.

	NRM Measurements			
Sample	Material	Dec°	Inc°	J(mAm^{-1})
5BA04	Tile	29.5	28.9	5110.1

5BA04.1	Tile	31.3	30.5	2571.6
5BA08	Tile	7.4	-12.3	3724.7
5BA09	Tile	3.7	-12.4	2700.2
5BA09.1	Tile	7.0	-12.2	3598.4
5BA10	Tile	4.7	-8.4	3518.7
5BA10.1	Tile	5.1	-5.5	1043.0
5BA11	Tile	-173.1	-6.2	1862.4
5BA12	Tile	-171.5	-4.0	1429.1
5BA13	Tile	-170.3	-4.0	1509.5
5BA14	Tile	-167.8	-4.0	1568.7
5BA14.1	Tile	-171.2	6.9	341.3

Table 12: NRM measurements of samples for feature 5BA. J = magnitude of magnetisation vector.

	5BA10		
AF(mT)	Dec°	Inc°	J(mAm^{-1})
0.0	4.7	-8.4	3518.7
1.0	4.3	-8.9	3491.3
2.5	3.6	-9.9	3463.3
5.0	3.6	-11.4	3300.3
10.0	3.5	-13.1	2713.7
15.0	3.4	-13.4	2219.9
20.0	3.8	-13.4	1874.3
30.0	3.8	-13.3	1531.7
50.0	4.7	-13.1	1127.7
75.0	4.4	-11.4	781.4
100.0	3.5	-10.3	595.2

Table 13: Incremental partial demagnetisation measurements for sample 5BA10.

Appendix: Standard Procedures for Sampling and Measurement

1) Sampling

One of three sampling techniques is employed depending on the consistency of the material (Clark, Tarling and Noel 1988):

a) **Consolidated materials:** Rock and fired clay samples are collected by the disc method. Several small levelled plastic discs are glued to the feature, marked with an orientation line related to True North, then removed with a small piece of the material attached.

b) **Unconsolidated materials:** Sediments are collected by the tube method. Small pillars of the material are carved out from a prepared platform, then encapsulated in levelled plastic tubes using plaster of Paris. The orientation line is then marked on top of the plaster.

c) **Plastic materials:** Waterlogged clays and muds are sampled in a similar manner to method 1b) above; however, the levelled plastic tubes are pressed directly into the material to be sampled.

2) Physical Analysis

a) Magnetic remanences are measured using a slow speed spinner fluxgate magnetometer (Molyneux et al. 1972; see also Tarling 1983, p84; Thompson and Oldfield 1986, p52).

b) Partial demagnetisation is achieved using the alternating magnetic field method (As 1967; Creer 1959; see also Tarling 1983, p91; Thompson and Oldfield 1986, p59), to remove viscous magnetic components if necessary. Demagnetising fields are measured in milli-Tesla (mT), figures quoted being for the peak value of the field.

3) Remanent Field Direction

a) The remanent field direction of a sample is expressed as two angles, declination (Dec) and inclination (Inc), both quoted in degrees. Declination represents the bearing of the field relative to true north, angles to the east being positive; inclination represents the angle of dip of this field.

b) Aitken and Hawley (1971) have shown that the angle of inclination in measured samples is likely to be distorted owing to magnetic refraction. The phenomenon is not well understood but is known to depend on the position the samples occupied within the structure. The corrections recommended by Aitken and Hawley are applied, where appropriate, to measured inclinations, in keeping with the practise of Clark, Tarling and Noel (1988).

c) Individual remanent field directions are combined to produce the mean remanent field direction using the statistical method developed by R. A. Fisher (1953). The quantity α_{95}, "alpha-95", is quoted with mean field directions and is a measure of the precision of the determination (see Aitken 1990, p247). It is analogous to the standard error statistic for scalar quantities; hence the smaller its value, the better the precision of the date.

d) For the purposes of comparison with standardised UK calibration data, remanent field directions are adjusted to the values they would have had if the feature had been located at Meriden, a standard reference point. The adjustment is done using the method suggested by Noel (Tarling 1983, p116).

4) Calibration

a) Material less than 3000 years old is dated using the archaeomagnetic calibration curve compiled by Clark, Tarling and Noel (1988).

b) Older material is dated using the lake sediment data compiled by Turner and Thompson (1982).

c) Dates are normally given at the 63% and 95% confidence levels. However, the quality of the measurement and the estimated reliability of the calibration curve for the period in question are not taken into account, so this figure is only approximate. Owing to crossovers and contiguities in the curve, alternative dates are sometimes given. It may be possible to select the correct alternative using independent dating evidence.

d) As the thermoremanent effect is reset at each heating, all dates for fired material refer to the final heating.

e) Dates are prefixed by "cal", for consistency with the new convention for calibrated radiocarbon dates (Mook 1986).

References

Aitken, M. J. 1990. *Science-based Dating in Archaeology*. London: Longman.

Aitken, M. J. and H. N. Hawley 1971. Archaeomagnetism: evidence for magnetic refraction in kiln structures. *Archaeometry* **13**, 83-85.

As, J. A. 1967. The a.c. demagnetisation technique, in *Methods in Palaeomagnetism*, D. W. Collinson, K. M. Creer and S. K. Runcorn (eds). Amsterdam: Elsevier.

Clark, A. J., D. H. Tarling and M. Noel 1988. Developments in Archaeomagnetic Dating in Britain. *J. Arch. Sci.* **15**, 645-667.

Creer, K. M. 1959. A.C. demagnetisation of unstable Triassic Keuper Marls from S. W. England. *Geophys. J. R. Astr. Soc.* **2**, 261-275.

Fisher, R. A. 1953. Dispersion on a sphere. *Proc. R. Soc. London A* **217**, 295-305.

IGRF, 2000. International Geomagnetic Reference Field - Epoch 2000. Revision of the IGRF for 2000 – 2005. *http://www.ngdc.noaa.gov/IAGA/wg8/igrf2000.html*

Molyneux, L., R. Thompson, F. Oldfield and M. E. McCallan 1972. Rapid measurement of the remanent magnetisation of long cores of sediment. *Nature* **237**, 42-43.

Mook, W. G. 1986. Recommendations/Resolutions Adopted by the Twelfth International Radiocarbon Conference. *Radiocarbon* **28**, M. Stuiver and S. Kra (eds), 799.

Tarling, D. H. 1983. *Palaeomagnetism*. London: Chapman and Hall.

Tarling, D. H. and Symons, D. T. A. 1967. A stability index of remanence in palaeomagnetism. *Geophys. J. R. Astr. Soc*. **12**, 443-448.

Thompson, R. and F. Oldfield 1986. *Environmental Magnetism*. London: Allen and Unwin.

Turner, G. M. and R. Thompson 1982. Detransformation of the British geomagnetic secular variation record for Holocene times. *Geophys. J. R. Astr. Soc.* **70**, 789-792.

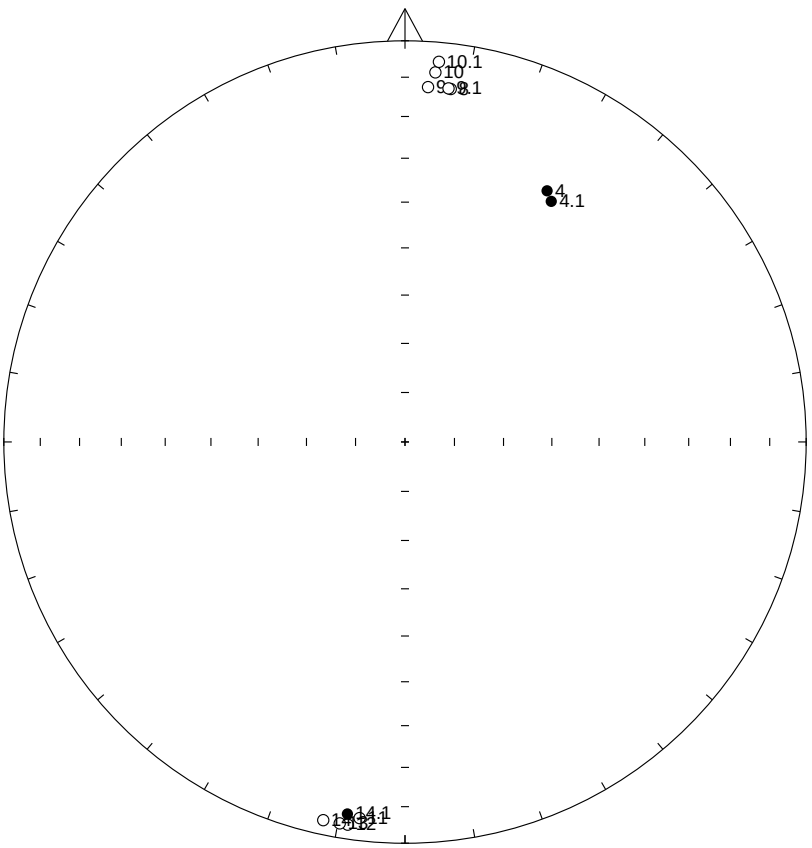

Figure 21: Distribution of NRM directions of samples from feature 5BA represented as an equal area stereogram. In this projection declination increases clockwise with zero being at 12 o'clock while inclination increases from zero at the equator to 90 degrees in the centre of the projection. Open circles represent negative inclinations.

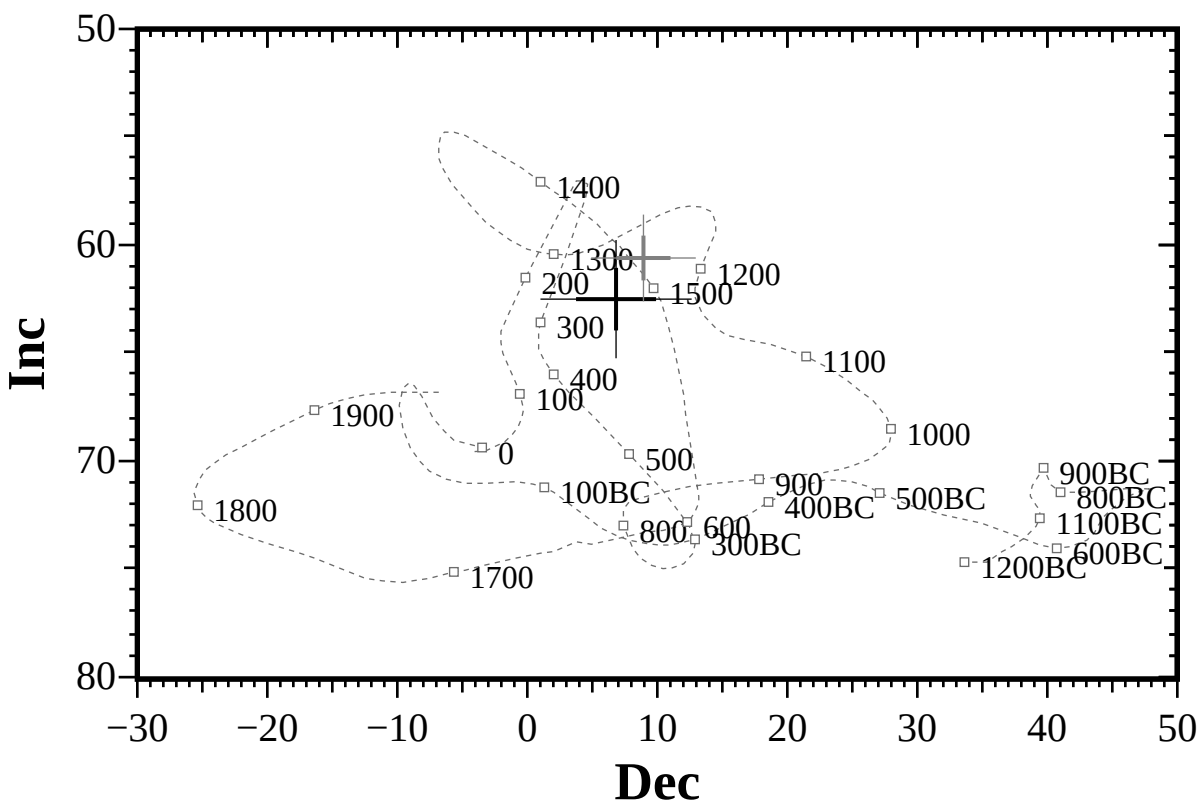

Figure 20: Comparison of the mean thermoremanent vector calculated from samples 01-04, 06, 07.1, 07.2 and 12-14 from feature 4BA after 15mT partial demagnetisation with the UK master calibration curve (black cross). The grey cross shows the mean thermoremanent direction of feature 2BA for comparison. Thick error bar lines represent 63% confidence limits and narrow lines 95% confidence limits.

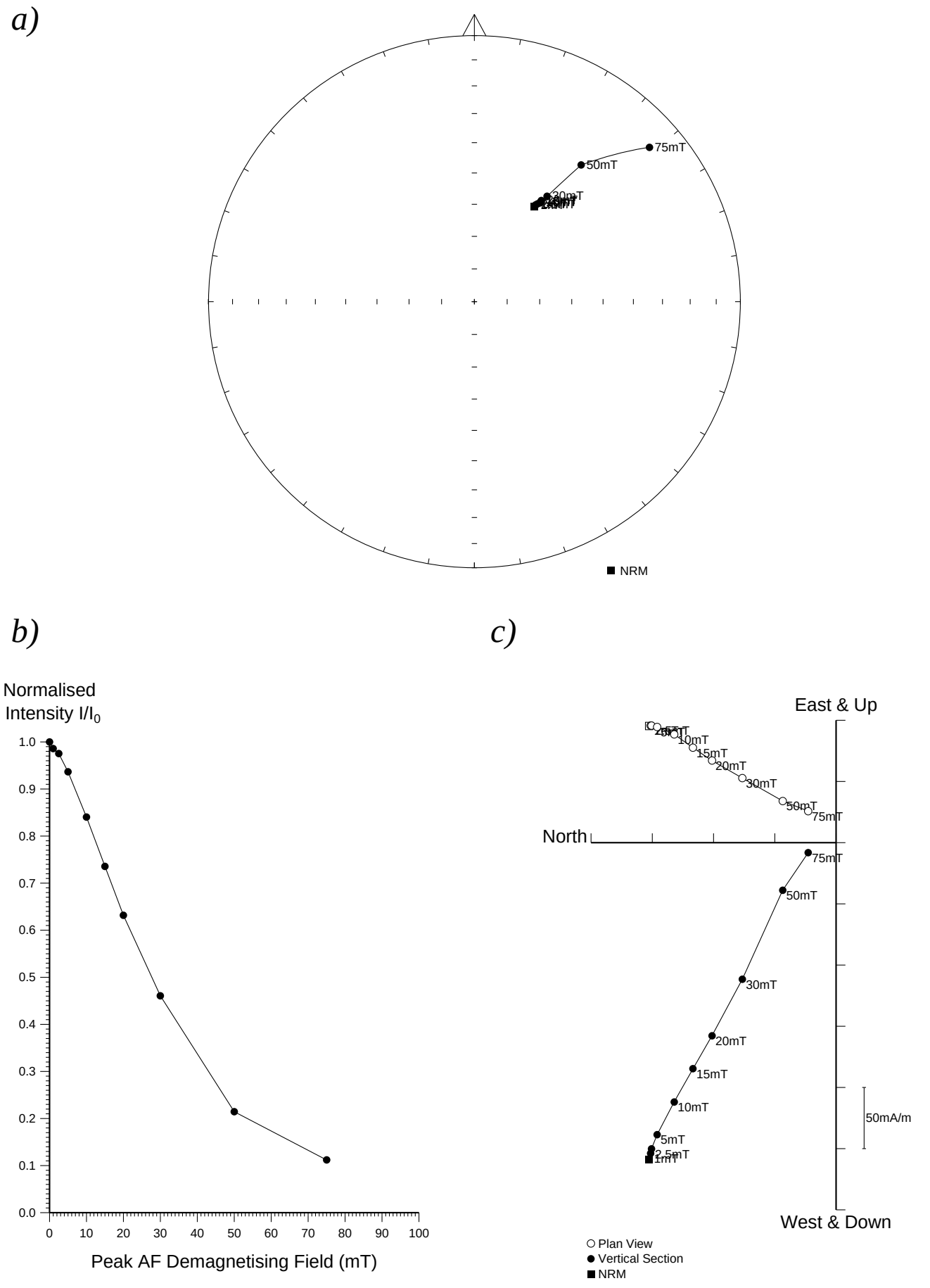

Figure 19: Stepwise AF demagnetisation of sample 4BA07.3. Diagram a) depicts the variation of the remanent direction as an equal area stereogram (declination increases clockwise, while inclination increases from zero at the equator to 90 degrees at the centre of the projection); b) shows the normalised change in remanence intensity as a function of the demagnetising field; c) shows the changes in both direction and intensity as a vector endpoint projection.

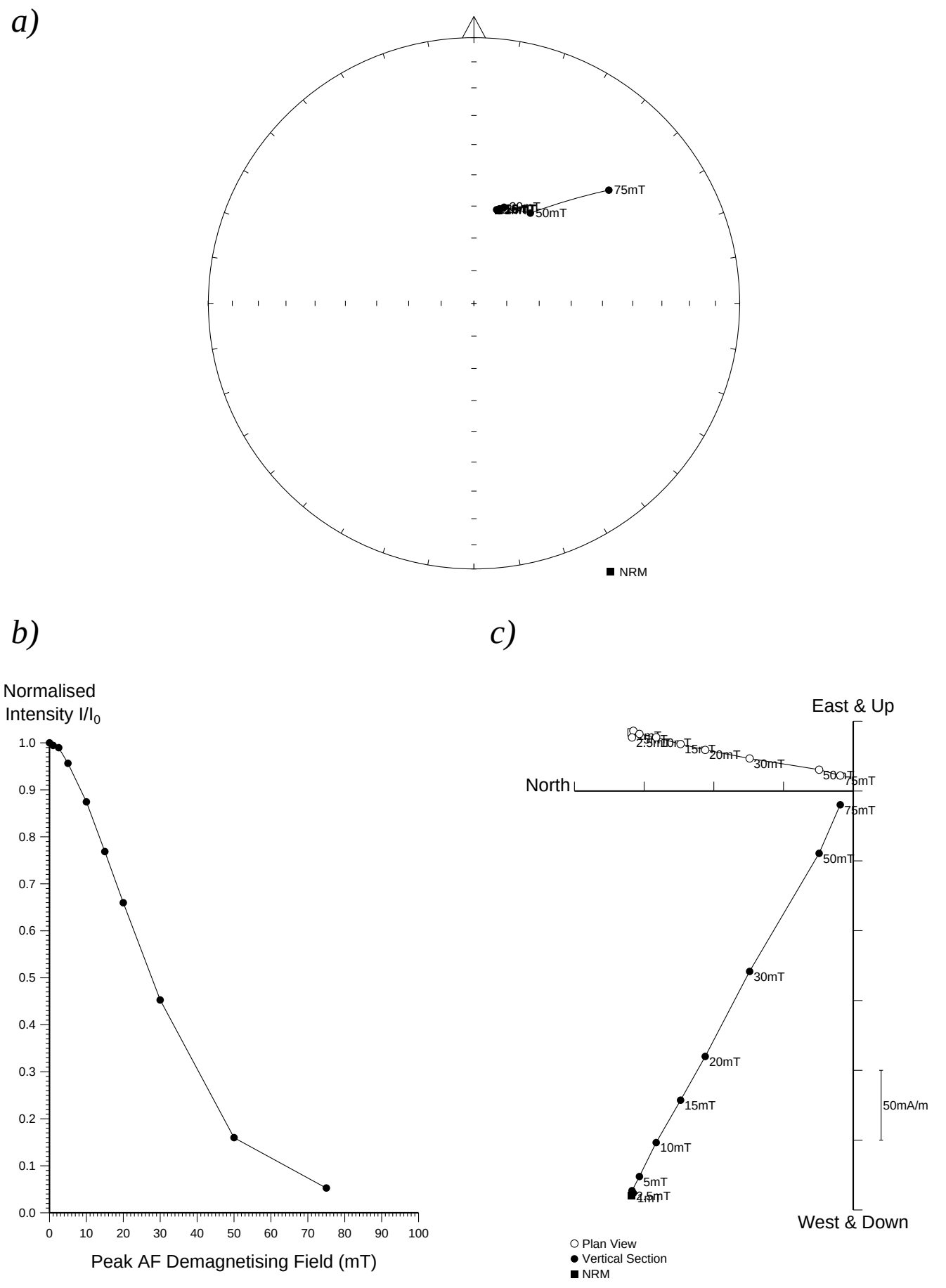

Figure 18: Stepwise AF demagnetisation of sample 4BA07.2. Diagram a) depicts the variation of the remanent direction as an equal area stereogram (declination increases clockwise, while inclination increases from zero at the equator to 90 degrees at the centre of the projection); b) shows the normalised change in remanence intensity as a function of the demagnetising field; c) shows the changes in both direction and intensity as a vector endpoint projection.

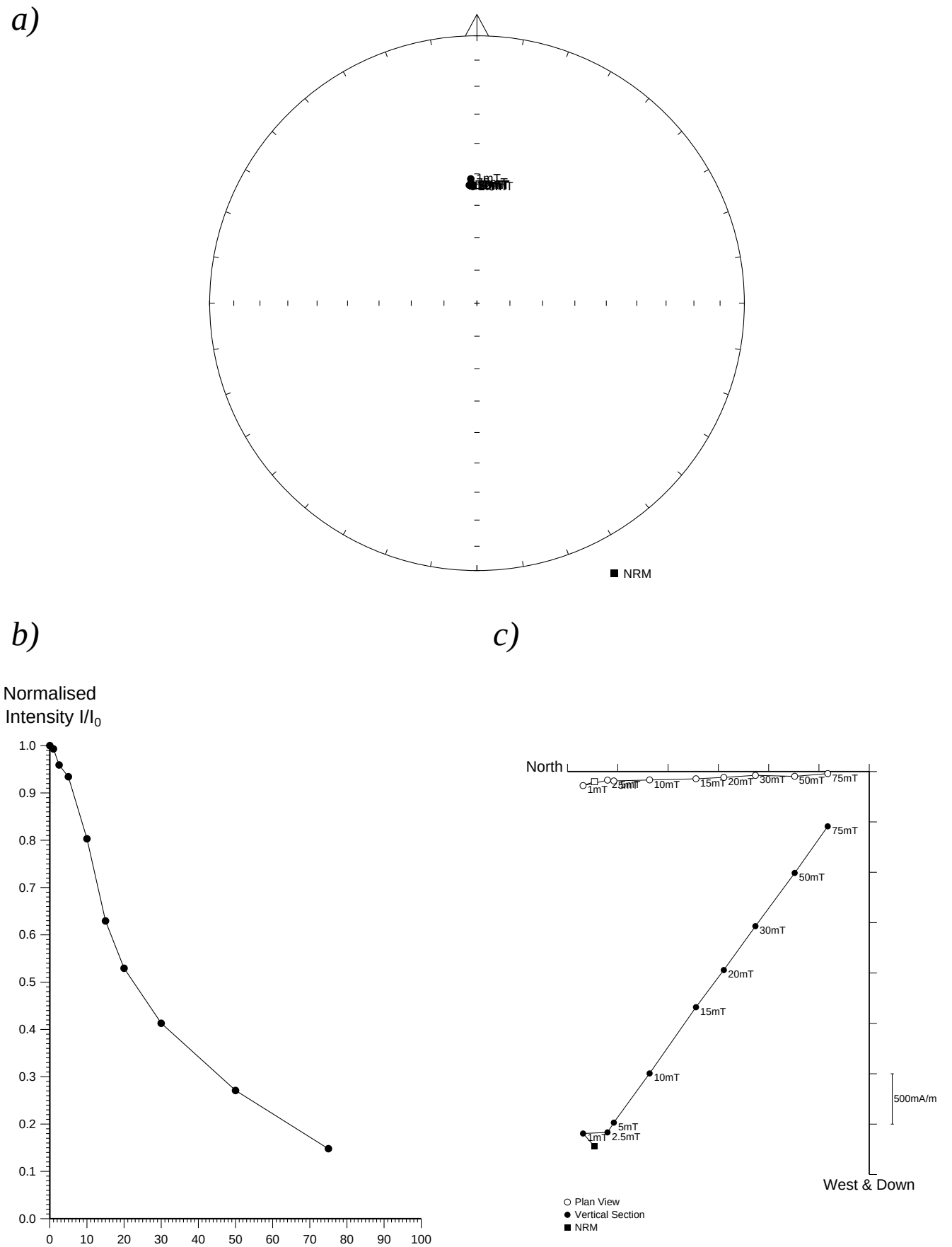

Figure 17: Stepwise AF demagnetisation of sample 4BA01. Diagram a) depicts the variation of the remanent direction as an equal area stereogram (declination increases clockwise, while inclination increases from zero at the equator to 90 degrees at the centre of the projection); b) shows the normalised change in remanence intensity as a function of the demagnetising field; c) shows the changes in both direction and intensity as a vector endpoint projection.

a)

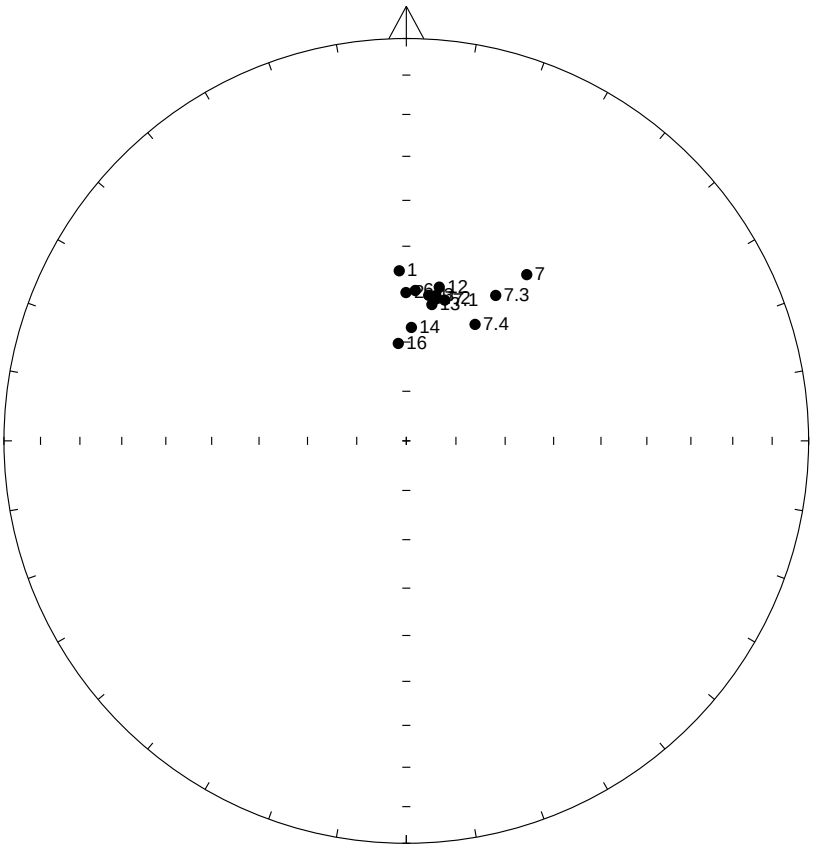

b)

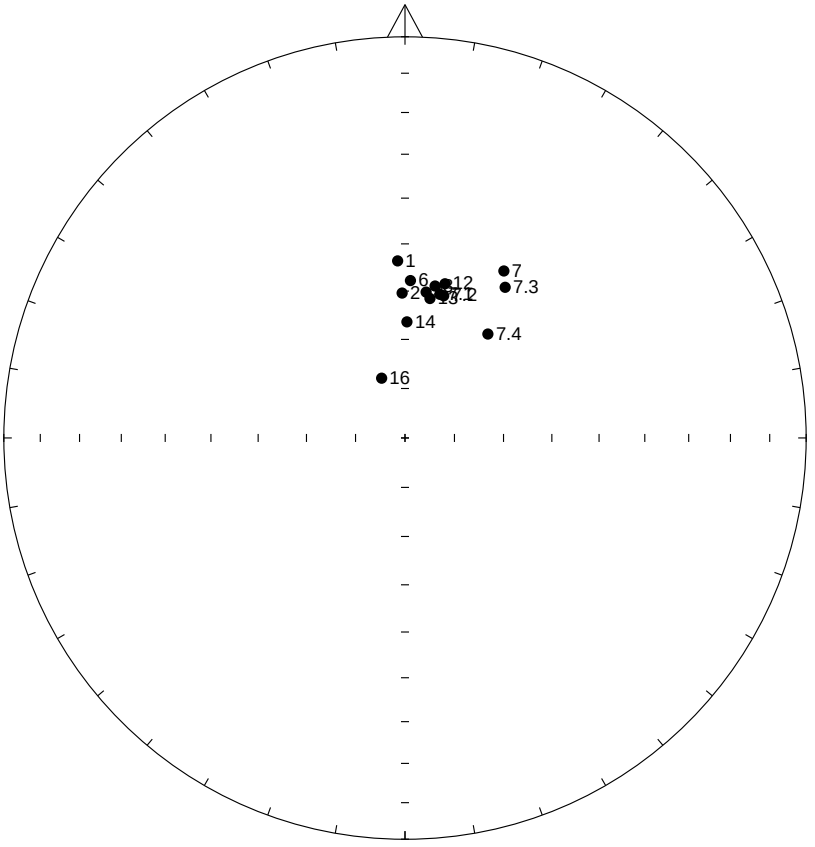

Figure 16: a) Distribution of NRM directions of samples from feature 4BA represented as an equal area stereogram. In this projection declination increases clockwise with zero being at 12 o'clock while inclination increases from zero at the equator to 90 degrees in the centre of the projection. Open circles represent negative inclinations. b) Distribution of thermoremanent directions of magnetisation of the same samples after partial AF demagnetisation to 15mT.

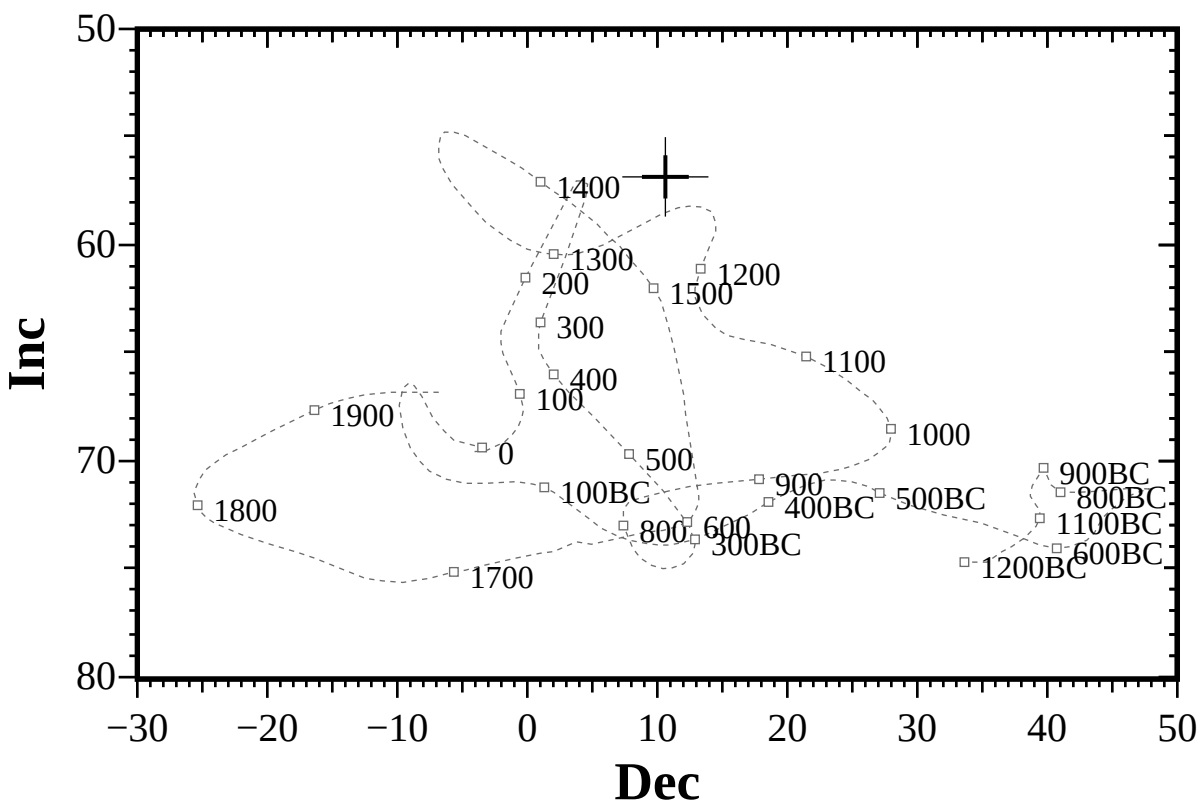

Figure 15: Comparison of the mean thermoremanent vector calculated from samples 01-09 and 13-17 from feature 3BA after 15mT partial demagnetisation with the UK master calibration curve. Thick error bar lines represent 63% confidence limits and narrow lines 95% confidence limits.

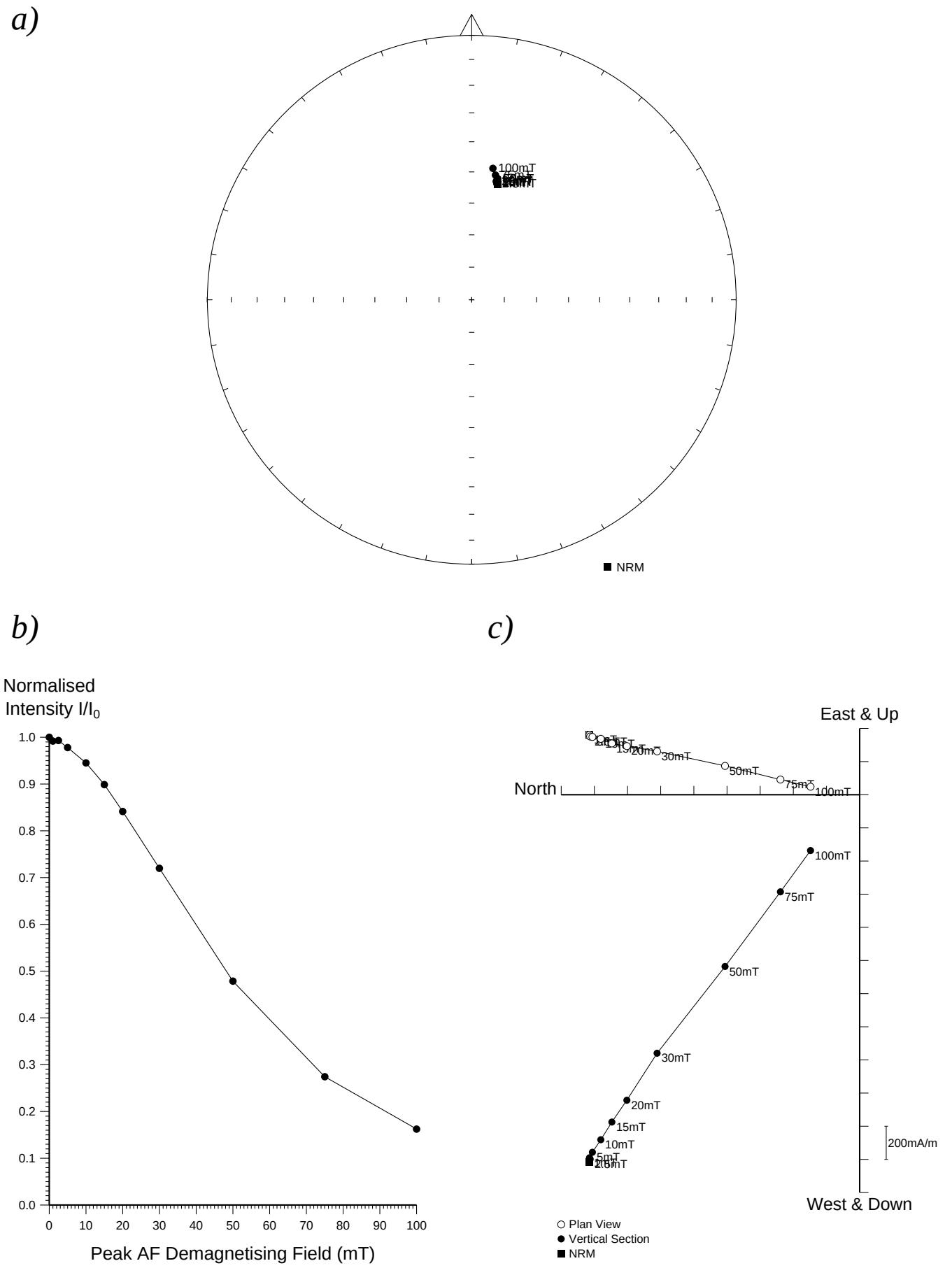

Figure 14: Stepwise AF demagnetisation of sample 3BA16. Diagram a) depicts the variation of the remanent direction as an equal area stereogram (declination increases clockwise, while inclination increases from zero at the equator to 90 degrees at the centre of the projection); b) shows the normalised change in remanence intensity as a function of the demagnetising field; c) shows the changes in both direction and intensity as a vector endpoint projection.

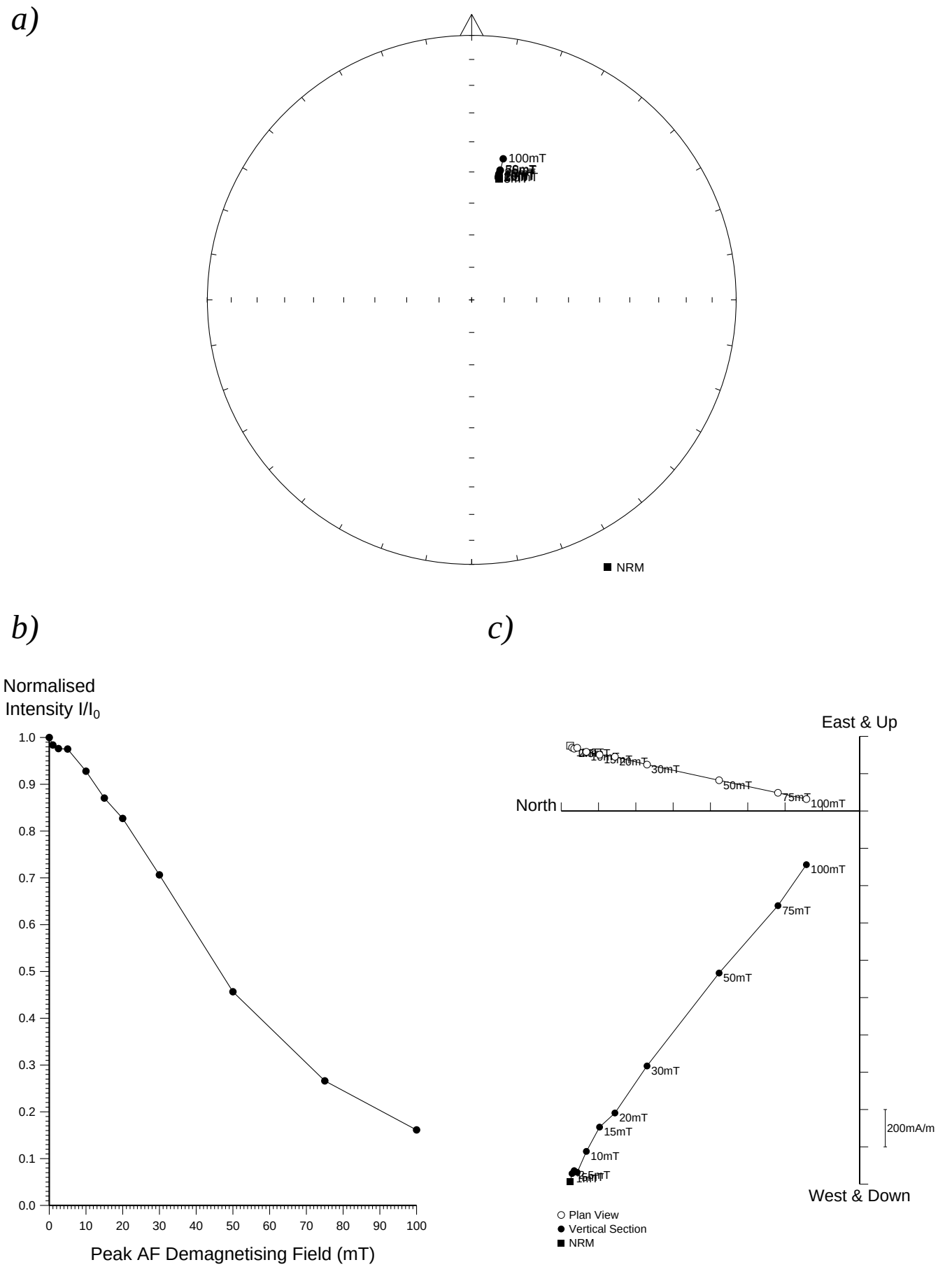

Figure 13: Stepwise AF demagnetisation of sample 3BA14. Diagram a) depicts the variation of the remanent direction as an equal area stereogram (declination increases clockwise, while inclination increases from zero at the equator to 90 degrees at the centre of the projection); b) shows the normalised change in remanence intensity as a function of the demagnetising field; c) shows the changes in both direction and intensity as a vector endpoint projection.

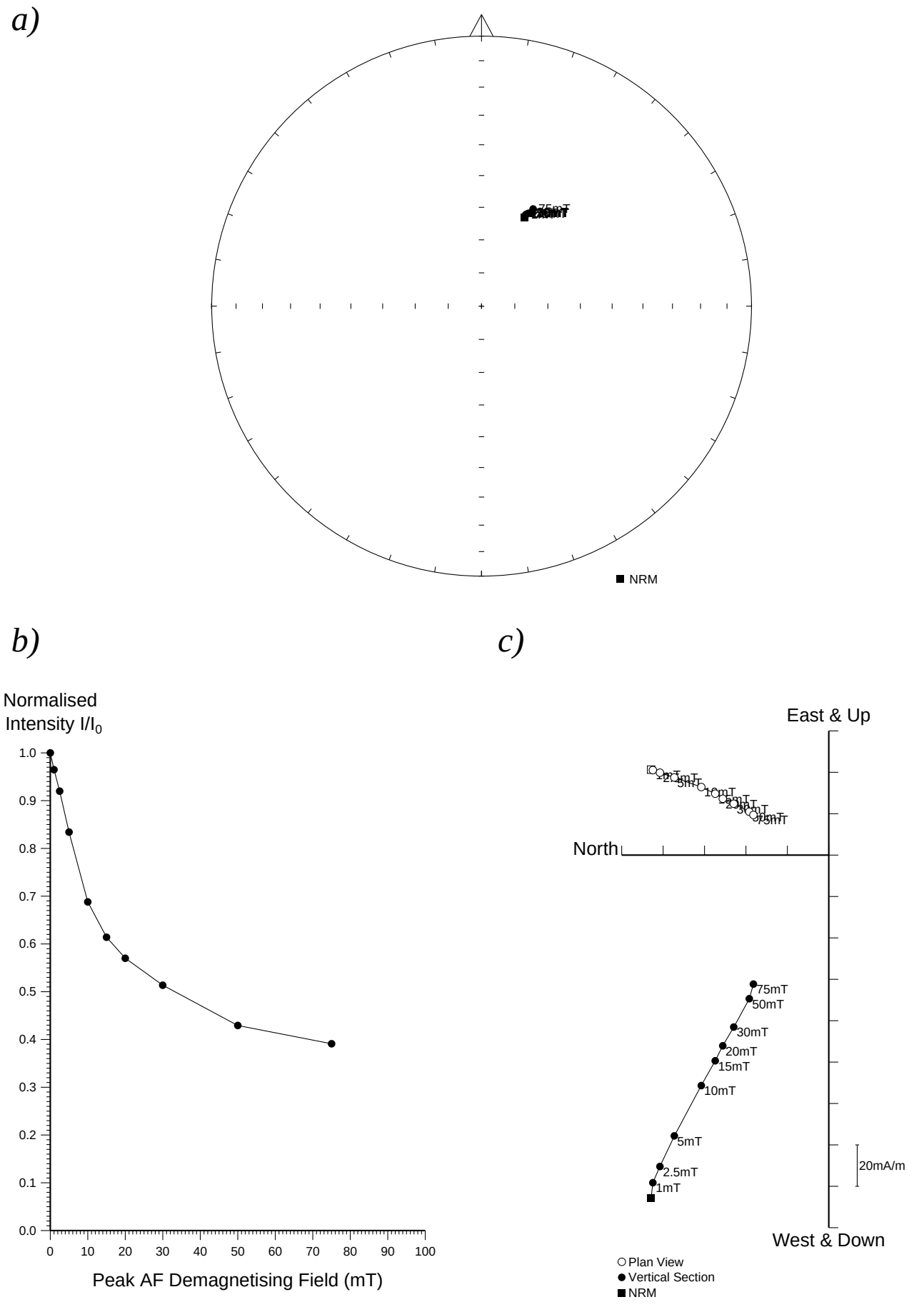

Figure 12: Stepwise AF demagnetisation of sample 3BA10. Diagram a) depicts the variation of the remanent direction as an equal area stereogram (declination increases clockwise, while inclination increases from zero at the equator to 90 degrees at the centre of the projection); b) shows the normalised change in remanence intensity as a function of the demagnetising field; c) shows the changes in both direction and intensity as a vector endpoint projection.

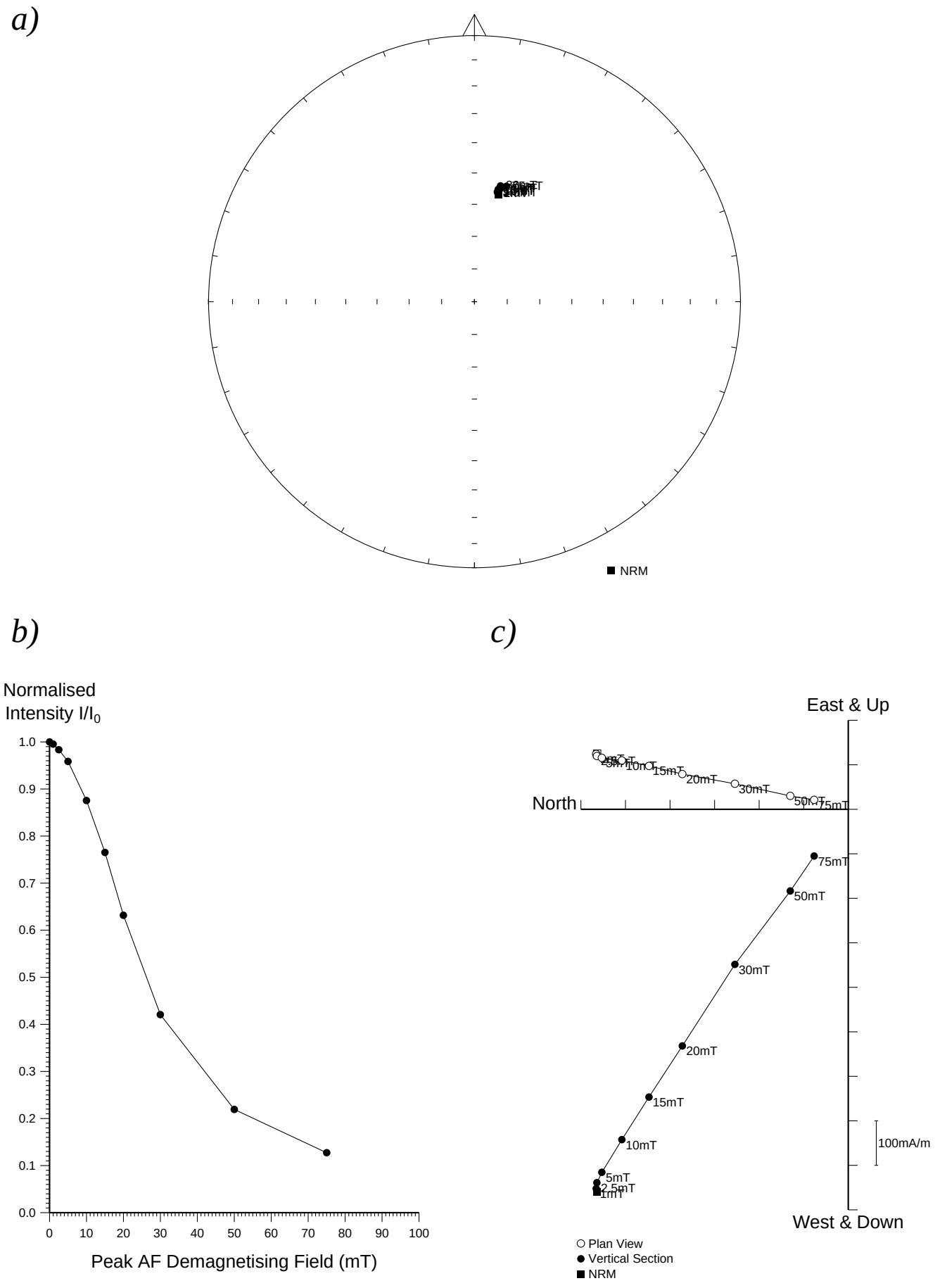

Figure 11: Stepwise AF demagnetisation of sample 3BA08. Diagram a) depicts the variation of the remanent direction as an equal area stereogram (declination increases clockwise, while inclination increases from zero at the equator to 90 degrees at the centre of the projection); b) shows the normalised change in remanence intensity as a function of the demagnetising field; c) shows the changes in both direction and intensity as a vector endpoint projection.

a)

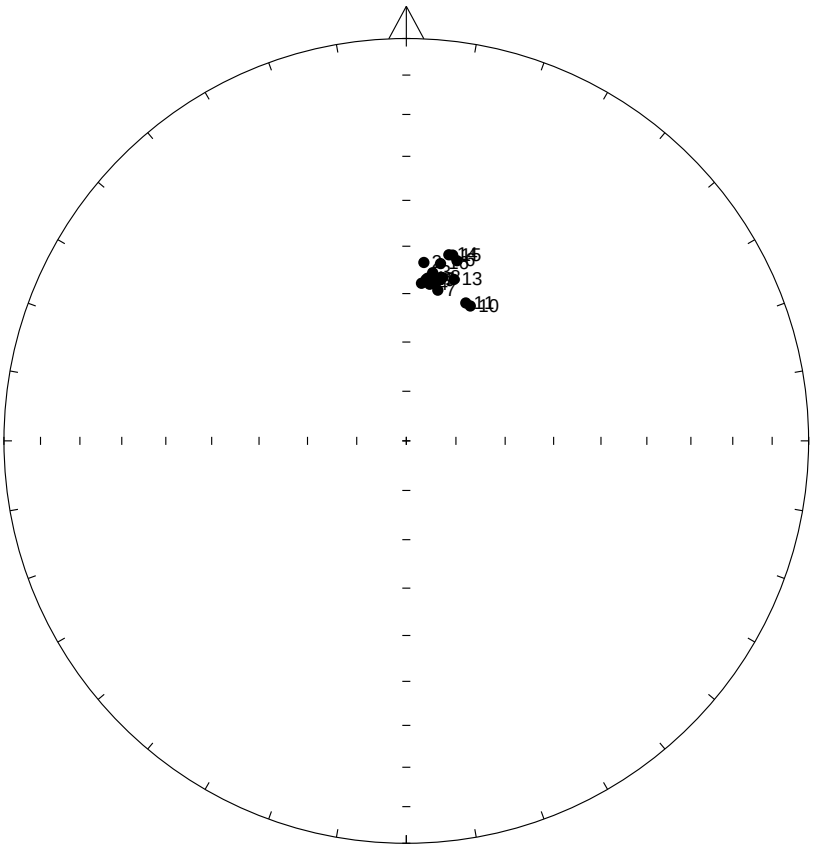

b)

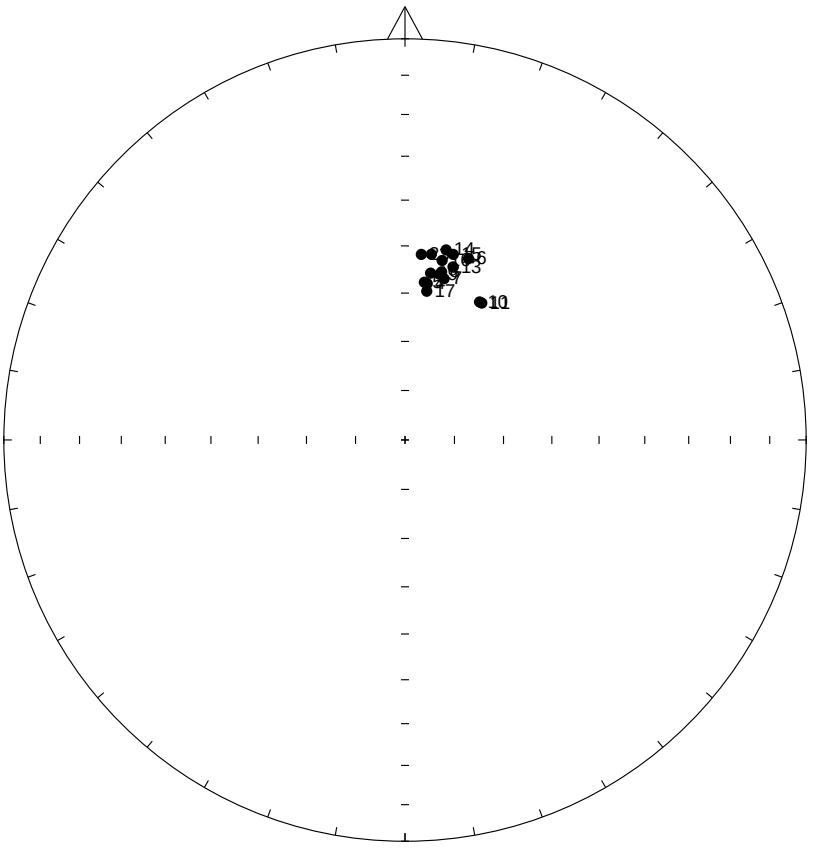

Figure 10: a) Distribution of NRM directions of samples from feature 3BA represented as an equal area stereogram. In this projection declination increases clockwise with zero being at 12 o'clock while inclination increases from zero at the equator to 90 degrees in the centre of the projection. Open circles represent negative inclinations. b) Distribution of thermoremanent directions of magnetisation of the same samples after partial AF demagnetisation to 15mT.

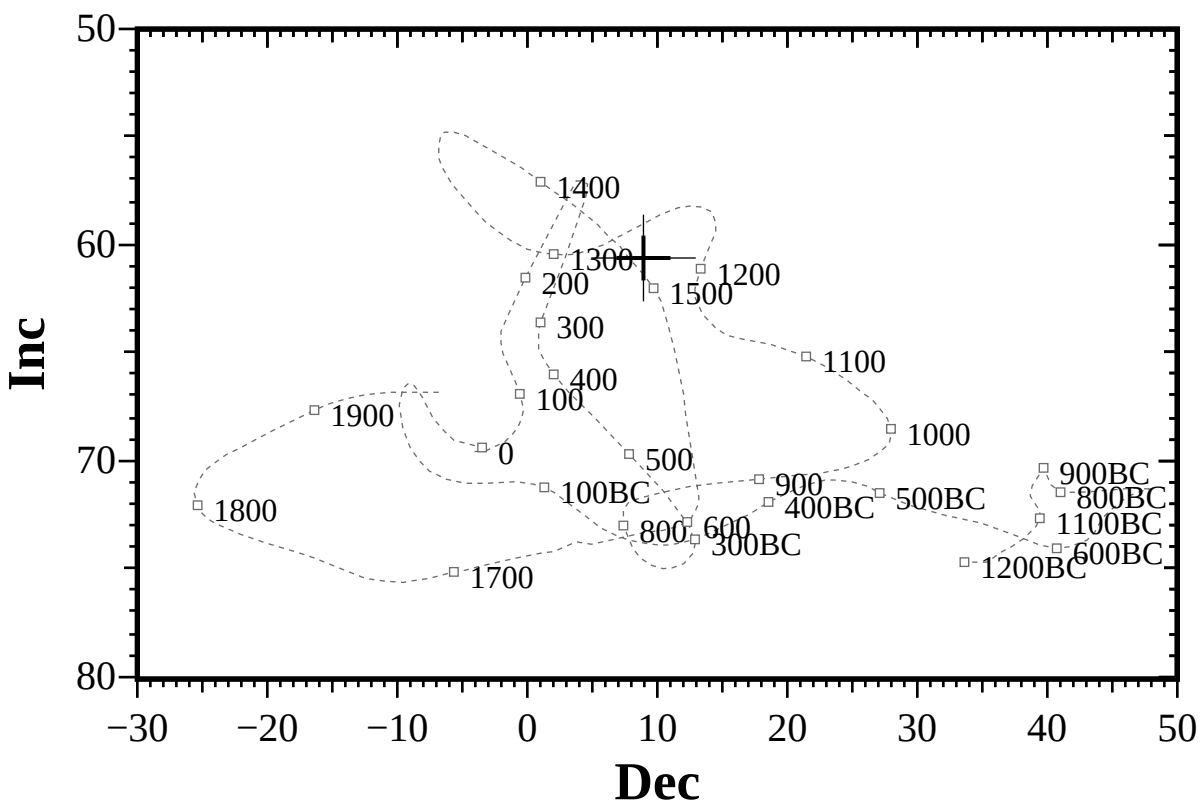

Figure 9: Comparison of the mean thermoremanent vector calculated from samples 03-05, 07-09 and 11-12 from feature 2BA after 15mT partial demagnetisation with the UK master calibration curve. Thick error bar lines represent 63% confidence limits and narrow lines 95% confidence limits.

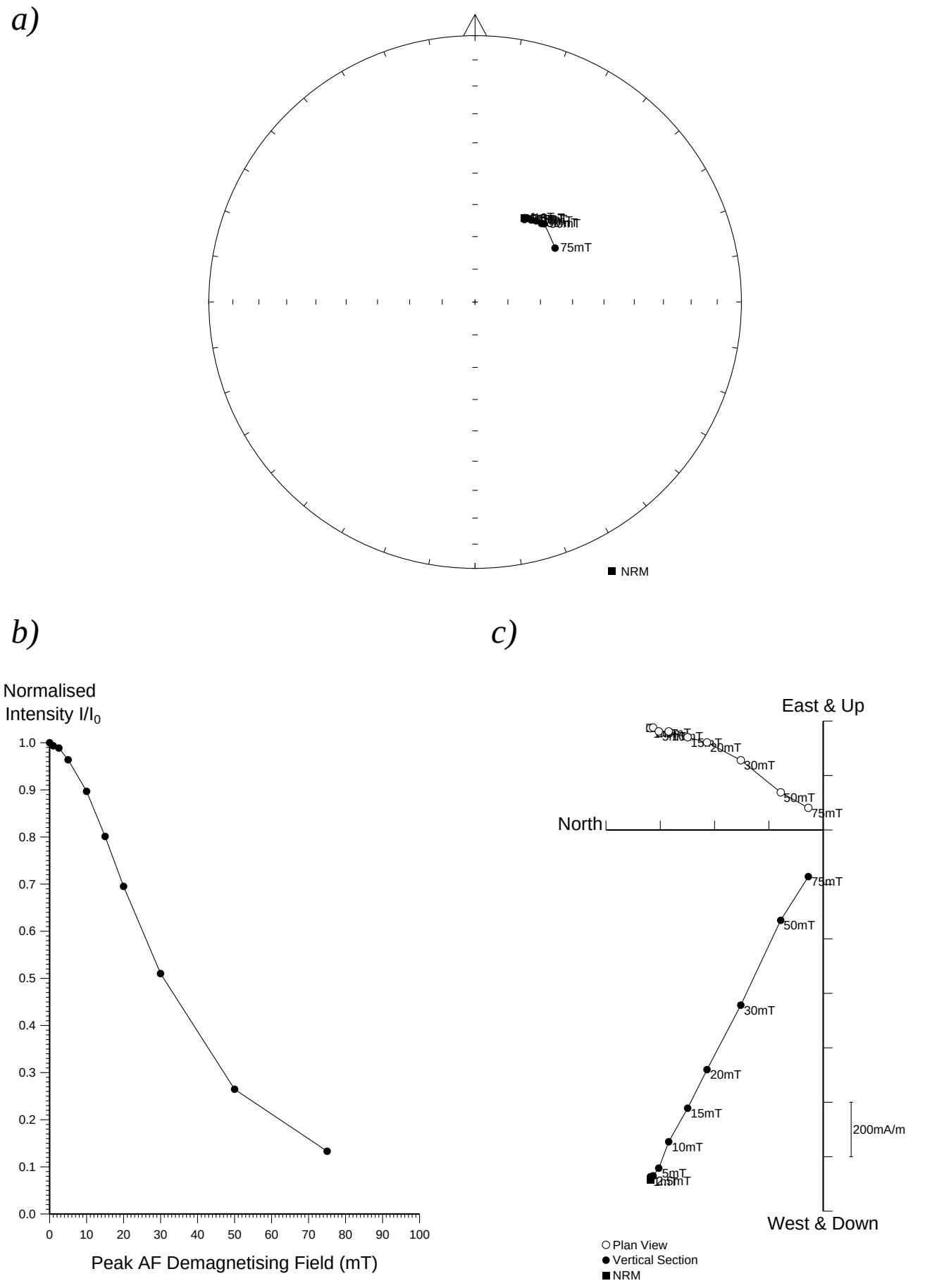

Figure 8: Stepwise AF demagnetisation of sample 2BA10. Diagram a) depicts the variation of the remanent direction as an equal area stereogram (declination increases clockwise, while inclination increases from zero at the equator to 90 degrees at the centre of the projection); b) shows the normalised change in remanence intensity as a function of the demagnetising field; c) shows the changes in both direction and intensity as a vector endpoint projection.

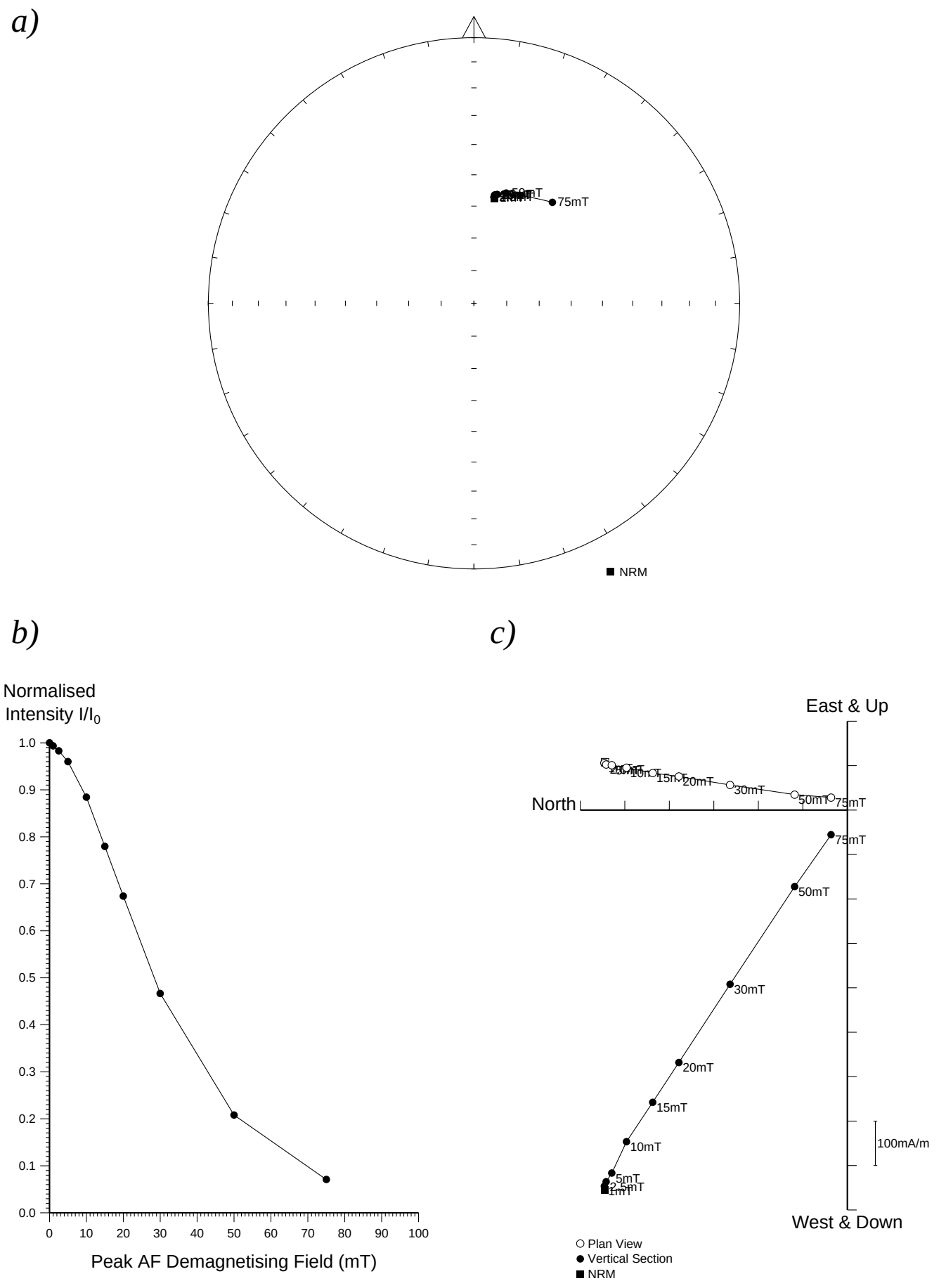

Figure 7: Stepwise AF demagnetisation of sample 2BA07. Diagram a) depicts the variation of the remanent direction as an equal area stereogram (declination increases clockwise, while inclination increases from zero at the equator to 90 degrees at the centre of the projection); b) shows the normalised change in remanence intensity as a function of the demagnetising field; c) shows the changes in both direction and intensity as a vector endpoint projection.

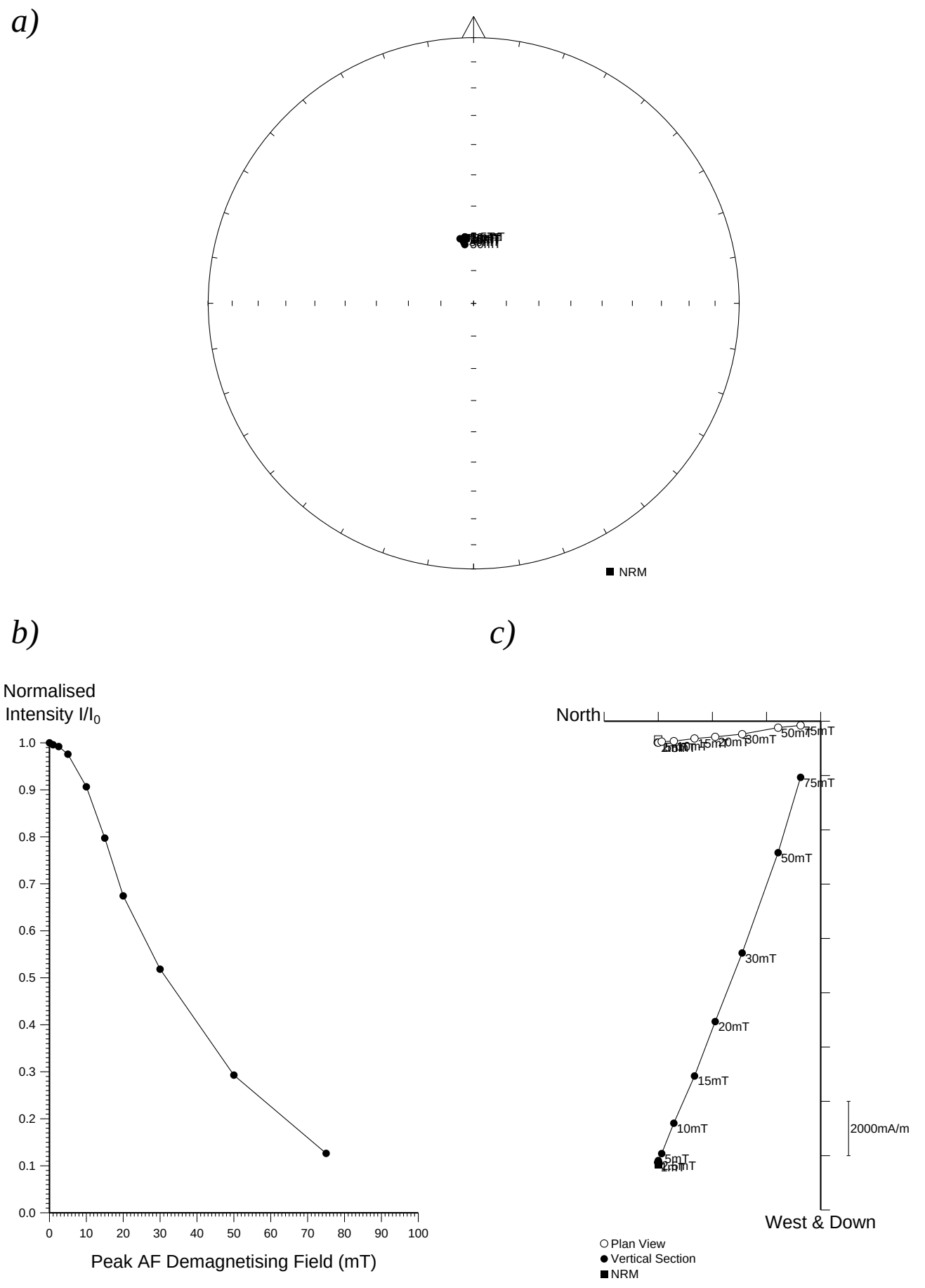

Figure 6: Stepwise AF demagnetisation of sample 2BA01. Diagram a) depicts the variation of the remanent direction as an equal area stereogram (declination increases clockwise, while inclination increases from zero at the equator to 90 degrees at the centre of the projection); b) shows the normalised change in remanence intensity as a function of the demagnetising field; c) shows the changes in both direction and intensity as a vector endpoint projection.

a)

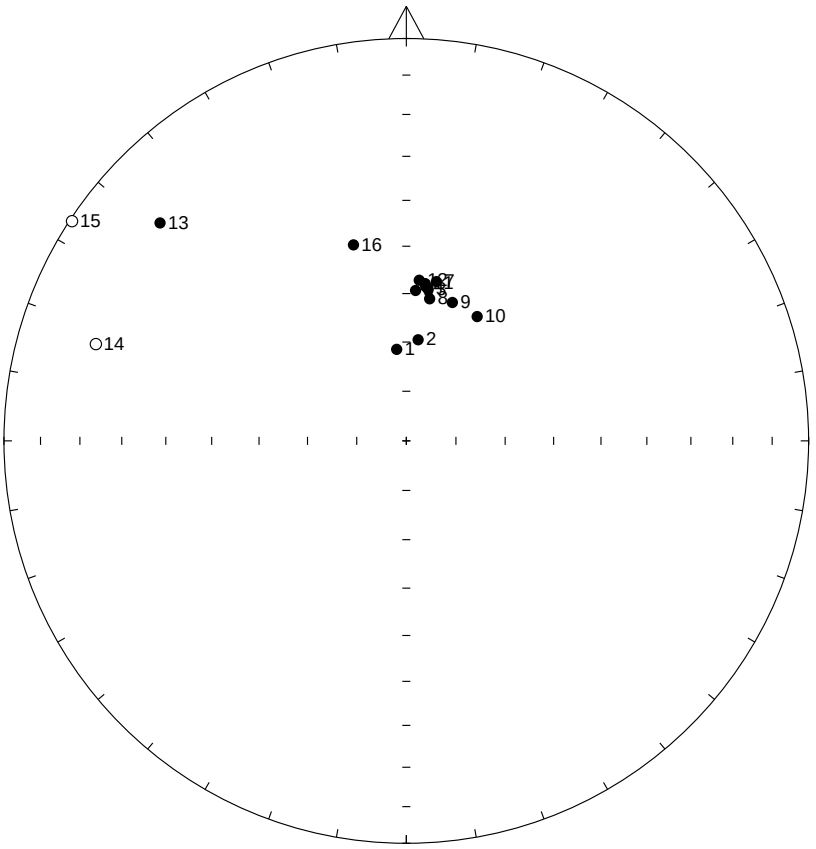

b)

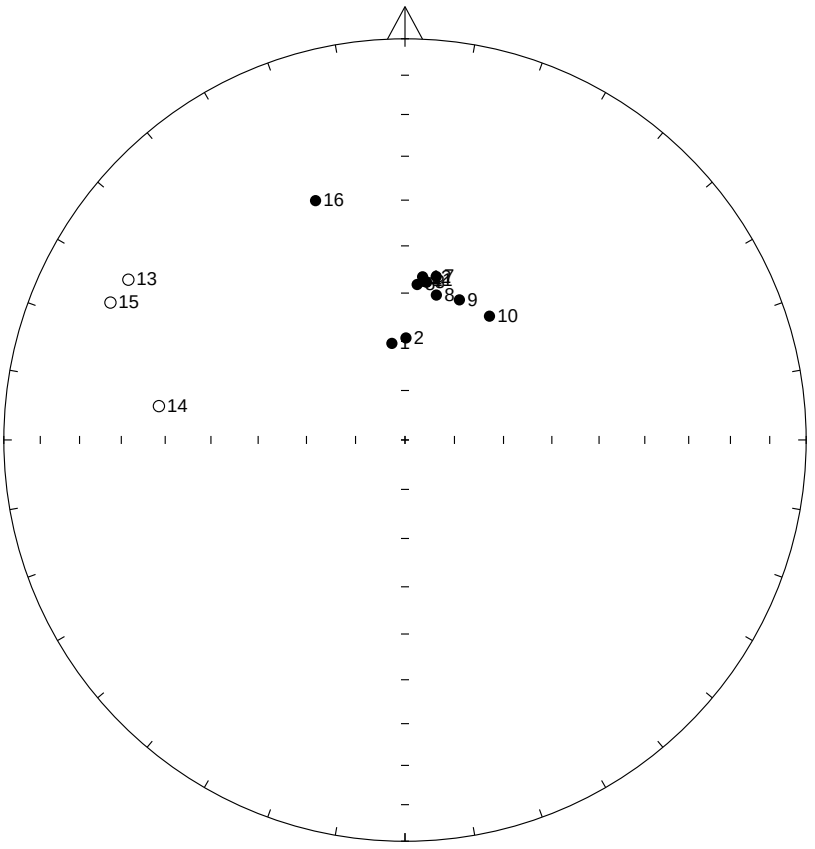

Figure 5: a) Distribution of NRM directions of samples from feature 2BA represented as an equal area stereogram. In this projection declination increases clockwise with zero being at 12 o'clock while inclination increases from zero at the equator to 90 degrees in the centre of the projection. Open circles represent negative inclinations. b) Distribution of thermoremanent directions of magnetisation of the same samples after partial AF demagnetisation to 15mT.

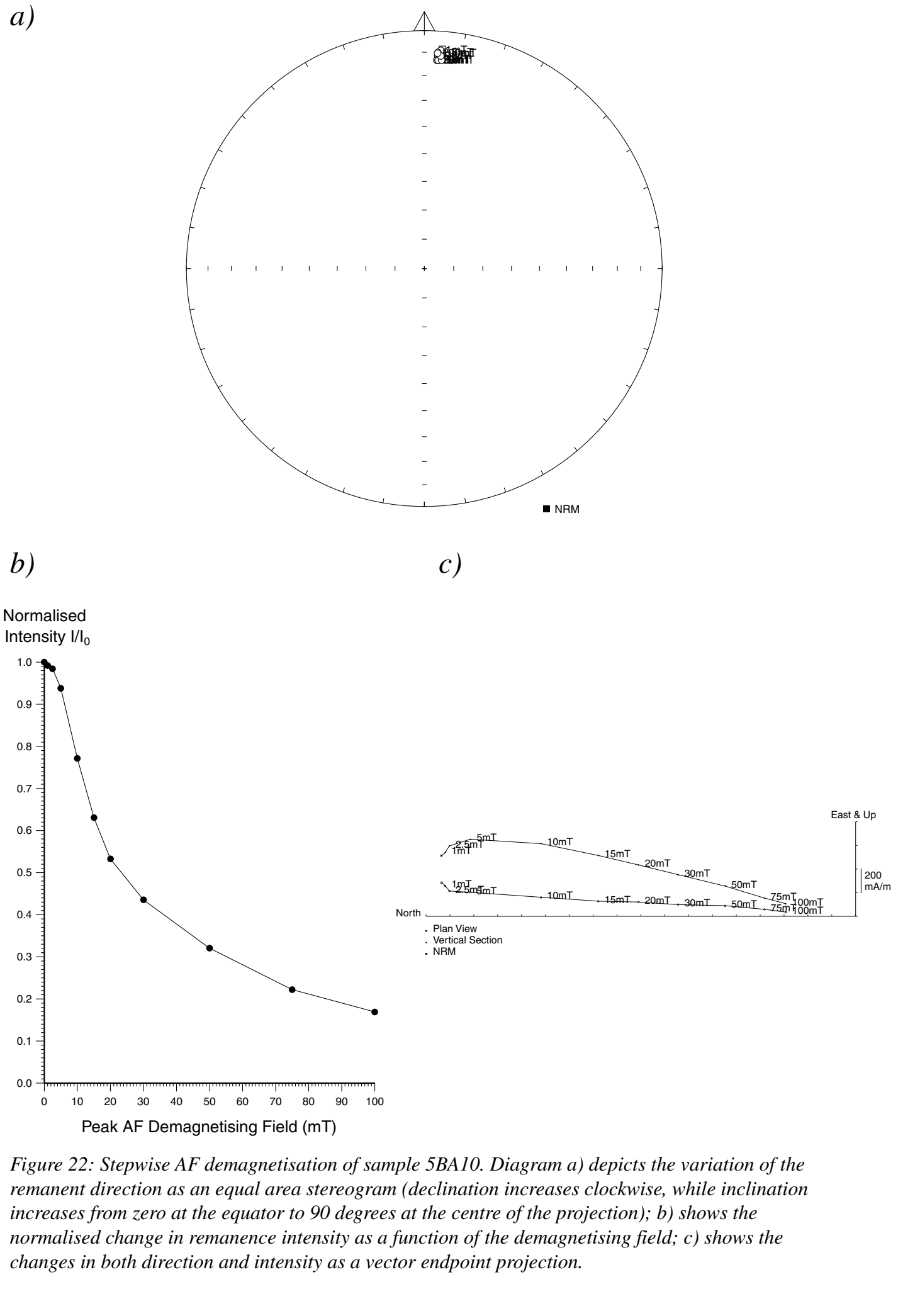

Figure 22: Stepwise AF demagnetisation of sample 5BA10. Diagram a) depicts the variation of the remanent direction as an equal area stereogram (declination increases clockwise, while inclination increases from zero at the equator to 90 degrees at the centre of the projection); b) shows the normalised change in remanence intensity as a function of the demagnetising field; c) shows the changes in both direction and intensity as a vector endpoint projection.